Semiclassical analysis
of the
Loop Quantum Gravity volume operator:
I. Flux Coherent States

C. Flori[1][*], T. Thiemann[1,2][†]

[1] MPI f. Gravitationsphysik, Albert-Einstein-Institut,
Am Mühlenberg 1, 14476 Potsdam, Germany

[2] Perimeter Institute for Theoretical Physics,
31 Caroline Street N, Waterloo, ON N2L 2Y5, Canada

Abstract

The volume operator plays a pivotal role for the quantum dynamics of Loop Quantum Gravity (LQG), both in the full theory and in truncated models adapted to cosmological situations coined Loop Quantum Cosmology (LQC). It is therefore crucial to check whether its semiclassical limit coincides with the classical volume operator plus quantum corrections.

In the present article we investigate this question by generalizing and employing previously defined coherent states for LQG which derive from a cylindrically consistently defined complexifier operator which is the quantization of a known classical function. These coherent states are not normalizable due to the non separability of the LQG Hilbert space but they define uniquely define cut – off states depending on a finite graph.

The result of our analysis is that the expectation value of the volume operator with respect to coherent states depending on a graph with only $n-$valent verticies reproduces its classical value at the phase space point at which the coherent state is peaked only if $n = 6$. In other words, the semiclassical sector of LQG defined by those states is described by graphs with cubic topology! This has some bearing on current spin foam models which are all based on four valent boundary spin networks.

[*]cecilia.flori@aei.mpg.de

[†]thiemann@aei.mpg.de,tthiemann@perimeterinstitute.ca

Contents

1 Introduction

The volume operator for Loop Quantum Gravity[1] (LQG) enters the quantum dynamics of the theory in a prominent way. Without it, Hamiltonian constraint operators [4], Master constraint operators [5] or physical Hamiltonian operators [6] cannot be defined. This is also true for truncated models of LQG such as Loop Quantum Cosmology (LQC) [7] which is supposed to describe well the homogeneous sector of the theory. In LQC one generically finds that the quantum evolution of operators corresponding to classically singular Dirac observables remain finite. This feature can be traced back to the way that inverse powers of the local volume, which enter into the expression for the triad, cotriad and other types couplings between geometry and geometry or geometry and matter, are quantized in the full theory [4]. Namely such derived operators are obtained as commutators between holonomy operators and powers of the volume operator.

In view of its importance, it is of outmost interest to verify that the classical limit of the LQG volume operator coincides with the classical volume. By this we mean that the expectation value of the volume operator with respect to suitable semiclassical states which are peaked on a given point in phase space coincides with the value of the classical volume at that phase space point up to small corrections and that its fluctuations are small.

Notice that there are actually two versions of the volume operator discussed in the literature [8, 9] which result from nonequivalent regularisations of the products of operator valued distributions that appear at intermediate stages. However, only the operator in [9] survives the consistency test of [10], namely that writing the volume in terms of triads which then are quantized using the above mentioned commutator, delivers the same operator up to $\hbar$ corrections as the direct quantization. This check is not unimportant as otherwise we should not trust the triad and cotriad quantisations that enter the quantum dynamics.

The semiclassical analysis of the volume operator has not been carried out yet although in principle suitable semiclassical (even coherent) states for LQG are available [11]. The reason for this is that the spectral decomposition (projection valued measure) of the volume operator cannot be computed exactly in closed form which however is needed in order to do exact practical calculations. More precisely, the volume operator is the fourth root of a positive operator Q whose matrix elements can be computed in closed form [12] but which cannot be diagonalized analytically. More in detail, the volume operator has discrete (that is, pure point) spectrum and it attains a block diagonal form where the blocks are labelled by the graphs and spin quantum numbers (labelling the edges of the graph) of spin network functions (SNWF) [13]. SNWF's form a convenient basis of the LQG Hilbert space [14] which is the unique (cyclic) Hilbert which carries a unitary representation of the spatial diffeomorphism group and the Poisson$^*-$algebra of the elementary (flux and holonomy) variables [15]. The blocks turn out to be finite dimensional matrices whose matrix elements[2] can be expressed in terms of polynomials of 6j symbols which fortunately can be avoided[2] using a telescopic summation technique [16] related to the Elliot – Biedenharn identity [17] so that a manageable closed expression results. However, the size of these matrices grows exponentially with increasing spin quantum numbers and since the expression for coherent states is a coherent superposition of SNWF's with arbitrarily large spin quantum numbers, a numerical computation of the expectation value using numerical diagonalisation techniques which are currently being developed [18] is so far out of reach[3]

The way to make progress is to use semiclassical perturbation theory developed in [19] and already applied in [20, 21]. The idea is quite simple: In practical calculations one needs the expectation value of Q^q where q is a rational number in the range $0 < q \leq \frac{1}{4}$. Introduce the "perturbation operator" $X := \frac{Q}{<Q>} - 1$ where the expectation value $< Q >$ of the positive operator Q is exactly computable. Notice that X is bounded from below by -1. Then trivially $< Q^q >=< Q >^q < [1 + X]^q >$. Now we use that there exist positive numbers p such that the classical estimates $1 + qx - px^2 \leq (1 + x)^q \leq 1 + qx$ are valid for all

---

[1]See [1, 2] for recent books and [3] for recent reviews.

[2]Notice that Racah's formula provides a closed expression for the 6j symbol but that it involves implicit sums and factorials involving large integers which quickly becomes unmanageable even numerically.

[3]The coherent superposition contains a damping factor which suppresses large spins and thus large matrices so that one may truncate the involved infinite series over spin quantum numbers at finite values making only negligible errors, but still the computational effort is currently too high for supercomputers, see e.g. the computation time estimates in reported [18].

$x \geq -1$. Finer estimates of this form involving arbitrary powers of x are also available [20]. In view of the spectral theorem, this classical estimate survives at the quantum level and we have $Y_- \leq Y \leq Y_+$ where $Y_+ = 1 + qX$, $Y_- = Y_+ - pX^2$, $Y = (1 + X)^q$. It follows that $< Y > \in [< Y_+ > -p < X^2 >, < Y_+ >]$. However, $< Y_+ >= 1$ and $< X^2 >= [< Q^2 > - < Q >^2]/ < Q >^2$ is proportional to the relative fluctuation of Q which of order of $\hbar$ [11]. It follows that to zeroth order in $\hbar$ we may replace $< Q^q >$ by $< Q >^q$ which is computable and whose error estimates are also computable as shown above.

While possible, the exact computation of $< Q >$, $< Q^2 >$, .. is still quite involved. Here the following result, proved in [11], is convenient: The computation of these expectation values (more generally for low order polynomials in flux operators) for $SU(2)$ spin network states coincide, to zeroth order in $\hbar$, with the corresponding calculations for $U(1)^3$ spin networks. On those, the volume operator is even diagonal. Hence we conclude that, as long as we are only interested in the zeroth order in $\hbar$ contribution, we may evaluate the expectation value of the volume operator for a fictive theory in which we may replace the non Abelian group $SU(2)$ by the Abelian group $(U1)^3$ which makes all calculations dramatically simpler.

The coherent states developed for LQG so far all have been constructed using the complexifier method reviewed in [22] which generalizes the coherent state construction for phase spaces that are cotangent bundles over compact groups developed in [23][4]. This involves the heat kernel evolution of the delta distribution (which is the matrix element of the unit operator in the Schrödinger (position) representation) with respect to a generalized Laplace operator, called the complexifier, followed by a certain analytic continuation. Now the unit operator in LQG can be written as a resolution of unity in terms of SNWF's and although the heat kernel is a damping operator, since the SNWF are not countable (the LQG Hilbert space is not separable), the resulting expression is not normalizable. It defines a well defined distribution (in the algebraic dual of the finite linear span of SNWF's) which can be conveniently written as a sum over cut – off states labelled by finite graphs. These states, called "shadows" in [23], *are* normalizable and one can use those in order to perform semiclassical calculations. Of course, one expects that only cut – off states labelled by graphs which are sufficiently fine with respect to the classical three metric to be approximated are good semiclassical states.

Hence we see that the input in the semiclassical calculations consists in the choice of a complexifier and the choice of a graph. One may wonder why the complexifier has to be chosen and is not dictated by the dynamics of the theory, that is, that the coherent states remain coherent under quantum time evolution (e.g. for the harmonic oscillator, the complexifier is strictly the Laplacian on the real line). The reason is twofold:

On the one hand one could perform constraint quantization and then we are working at the level of the kinematical Hilbert space on which the quantum constraints have not been imposed yet and all we want to make sure is that the volume operator, which is not gauge invariant (and thus does not preserve the physical Hilbert space) has a good classical limit on the kinematical Hilbert space (we would not trust a constraint quantization for which not even that was true).

On the other hand, one could also work at the level of the physical Hilbert space as outlined in [6] and then one would expect that the time evolution of any reasonable choice of complexifier coherent states with respect to the physical Hamiltonian defined there remains coherent (and peaked on the classical trajectory) for sufficiently short time intervals. Notice that for interacting theories as simple as the an-harmonic oscillator globally stable coherent states have so far not been found.

The choice of the complexifier will be guided by practical considerations, namely that it be diagonal on SNWF's and that it is a damping operator which makes the heat kernel evolution of the delta distribution restricted to a graph normalizable. Moreover, it should be gauge invariant under the $SU(2)$ gauge group. As far as the choice of the graph is concerned, for practical reasons one will choose graphs that are topologically regular, that is, have constant valence for each vertex. Indeed, the semiclassical calculations performed in [20, 21] were done using graphs of cubic topology with good semiclassical results.

The existing literature on such coherent states for LQG can be divided into two classes, depending on a certain structure that defines them:

---

[4]See also [24] for related ideas valid for Abelian gauge theories such as Maxwell theory or linearized gravity.

On the one hand, there are *gauge covariant flux* coherent states which depend on collections of surfaces and path systems inside them [11]. On the other hand, there are *area* coherent states which only depend on collections of surfaces but involve area operators rather than flux operators [22]. We will review and generalize both constructions. In its most studied incarnations, the collection of surfaces involved in [11] is defined by a polyhedronal partition of the spatial manifold while the collection involved in [22] is in terms of a parquette of foliations of the spatial manifold.

The novel results of this article are as follows:

1. *Cylindrically consistent complexifier*

   The important thing to notice is that both constructions are cylindrically consistent: Both derive from a complexifier which is graph independently defined in terms of the surfaces (and path systems) only and has consistent cylindrical projections to spin network functions over any graph. We stress this, because from the discussion in [11] one may get the impression that the states constructed there do not come from a single complexifier operator. We clarify this in this paper by explicitly constructing those projections. The apparent contradiction is resolved by observing that in [11] cut – off states were displayed only for graphs which are dual to a fixed polyhedronal complex. In this paper we treat the general case which is more complicated. We also give a compact expression for the eigenvalues of the complexifier of type [22] which is missing there.

2. *Graphs of arbitrary valence*

   The real motivation for the present article is that the calculations performed in [20, 21] raised the suspicion that the volume operator attains acceptable coherent state expectation values only for graphs of cubic topology. Therefore in this paper we perform the semiclassical analysis with respect to topologically regular graphs of valence n with $n = 4, 6, 8$. Ideally one would like to treat the general case but this leads to complicated book keeping problems. Fortunately, the cases we consider turn out to be sufficient to answer the afore posed question.

The outcome of our analysis is that, no matter whether one uses the states [11] or [22], *the correct semiclassical limit is attained with these states for $n = 6$ only.* In other words:

Up to now, there are no semiclassical states known for other than cubic graph topology!

We interpret this result as saying that the states we constructed are simply not semiclassical for the volume operator unless $n = 6$. The ratio consisting of expectation value of the volume operator with respect to the coherent states for graphs of valence $n \neq 6$ divided by the classical value deviates from unity by a geometrical factor q_n depending on n which is of order unity and not at all of order $\hbar$. One might argue that therefore one should rescale the volume operator by $1/q_n$. However, first of all this is not allowed because the normalization is fixed [10] and secondly even if one would rescale, the statement would still be that the correct expectation value is attained for a unique valence only.

It may be that there are other semiclassical states coming from a different complexifier or from an entirely different method which does not have this problem. However, notice that all coherent states that were constructed so far for free field theories on Minkowski space come from a complexifier, so the complexifier method is natural and well tested in other contexts [22]. Secondly, as shown in [22], the choice of a SU(2) invariant and background metric invariant complexifier for LQG with computable spectrum and the required damping behavior leaves relatively little possibilities and to the best of our knowledge, the states proposed in [11, 22] and used here are the simplest and only ones known so far. Therefore, even if better suited states exist, they will be very hard to guess and even harder to do practical calculations with.

The implication of our result for LQG then seems to be that the semiclassical sector of the theory is spanned by SNWF based on cubic graphs. This has some bearing for spin foam models [26] which are supposed to be – but have so far not been proved to be – the path integral formulation of LQG. Spin foams are certain state sum models based on simplicial triangulations of four manifolds whose dual graphs are therefore five valent. Since the intersection of this graph with a boundary three manifold is therefore four valent, we see that spin foam models based on simplicial triangulations corresponds to boundary Hilbert

spaces spanned by spin network states based on four valent graphs only[5].

But even if these mismatches between LQG and spin foams could be surmounted, the result of our analysis seems to say that *the boundary Hilbert space of current spin foam models does not contain any semiclassical states!* This seems to contradict recent findings that the graviton propagator derived from spin foam models comes out correctly [31]. However, notice that these results only show that the propagator comes out with the correct fall off behavior while the correct tensorial structure has not been verified yet. An easy way to possibly repair this is to generalize spin foam models and allow for arbitrary, in particular cubic, triangulations as suggested in [32, 33].

The outline of this paper is as follows:

In section two we review the general complexifier method and generalize the complexifier coherent states proposed in [11, 22]. In particular, we review the two families of coherent states introduced so far which are based on complexifiers constructed from squares of flux or area operators respectively. We also explicitly compute the corresponding cut – off states for SU(2) and show when and why it is justified to work with a fictive $U(1)^3$ theory instead as far as the zeroth order in $\hbar$ for the expectation values is concerned.

In section three we construct explicitly convenient tetrahedronal, cubical and octaheronal cell decompositions of the spatial manifold which also define regular dual $n = 4, 6, 8$ valent dual graphs. These constructions are needed for the explicit calculations in section four and for our companion paper [34].

In section four we compute the expectation value of the volume operator for the constant valence cases $n = 4, 6, 8$ for the states of type [11]. We will do the same in our companion paper [34] for the states of type [22]. In addition, in [34] we answer the following question: While the flux complexifier is built from a discrete set of fluxes, the area complexifier is built from a continuous set of areas whose underlying surfaces fill all of space. While this makes the calculations more cumbersome, it might improve the quality of the corresponding coherent states in the sense that the expectation values do not strongly depend on the cut – off graph chosen (as already mentioned above, at least when the graph has cubic topology). Hence, we examine the question whether the expectation value of geometrical operators is invariant under Euclidean transformations of the graph in case that the spatial metric to be approximated is Euclidean.

In section five we summaries and conclude.

2 Complexifier Coherent States

In this section we review the complexifier method to construct coherent states. We will be brief, all details can be found in [22] and references therein. This section is divided into six parts:
In the first we define the general complexifier framework. In the second we provide natural gauge invariant choices of complexifiers for background independent SU(2) gauge theories such as General Relativity and fictive $U(1)^3$ gauge theories. In the third we compute the associated coherent states. These are not normalizable because they involve a sum over an uncountable set of graphs but one can extract from them normalizable states in which the sum over all graphs is cut off to a finite number and which we display in the fourth part. In the fifth part we compare the properties of the states [11] and [22]. Finally, in the sixth we show that as far as the zeroth order in $\hbar$ is concerned, we may replace the complicated $SU(2)$ calculations by the much simpler $U(1)^3$ calculations under certain restrictions on the cut – off graph. This approximation is needed only for states of type [22]. For the states of type [11] it is sufficient to take as a cut – off graph

---

[5] As an aside, whether this boundary Hilbert space of spin foams really can be interpreted as the four valent sector of LQG is a subject of current debate even with the recent improvement [27] of the Barrett – Crane model [28] mostly studied so far. There are two problems: First, the boundary connection predicted by spin foams does not coincide with the LQG connection [29]. Secondly, the four valent sector of the LQG Hilbert space is not a superselection sector for the holonomy flux algebra of LQG. In fact, the LQG representation is known not only to be a cyclic but even an irreducible representation [30]. Therefore the four valent sector is not invariant under the LQG algebra.

any graph which is dual to the polyhedronal complex that defines the complexifier.

2.1   General Complexifier Method

We consider a symplectic manifold $\mathcal{M} = T^*(\mathcal{C})$ which is a cotangent bundle over a configuration manifold $\mathcal{C}$ which may be infinite dimensional (we will suppress any indices in what follows).

Definition 2.1.
A complexifier $C : \mathcal{M} \to \mathbb{R}^+$ is a sufficiently smooth, positive function on $\mathcal{M}$ with dimension of an action which has the following scaling behavior

$$\lim_{\lambda \to \infty} \frac{C(q, \lambda p)}{\lambda} = \infty \tag{2.1}$$

where (q, p) are the canonically conjugate, real configuration and momentum coordinates on $\mathcal{M}$.

The reasons for these restrictions become evident in a moment. With the aid of C we define

$$z := \exp(-i\{C, .\}) \cdot q = \sum_{n=0}^{\infty} \frac{(-i)^n}{n!} \{C, q\}_{(n)} \tag{2.2}$$

with inductively defined multiple Poisson brackets $\{C, f\}_{(0)} := f$, $\{C, f\}_{(n+1)} := \{C, \{C, f\}_{(n)}\}$. The meaning of "sufficiently smooth" is that all coefficients in the Taylor expansion (2.2) exist. Notice that (2.2) defines a (complex valued) canonical transformation whence $\{z, z\} = \{\bar{z}, \bar{z}\} = 0$ (this is non trivial when $\dim(\mathcal{C}) \geq 2$). The scaling behavior implies that z, $\bar{z}$ can be used as coordinates for $\mathcal{M}$. In fact, $z \in \mathcal{C}^{\mathbb{C}}$ defines a complex polarization of $\mathcal{M}$.

We now assume that $\mathcal{M}$ can be quantized, that is, there is a representation $(q, p) \mapsto (\hat{q}, \hat{p})$ of the Poisson* algebra defined by $\{q, q\} = \{p, p\} = 0$, $\{p, q\} = 1_{\mathcal{M}}$; $\bar{q} = q$, $\bar{p} = p$ on a Hilbert space of the form $\mathcal{H} = L_2(\overline{\mathcal{C}}, d\mu)$ where $\overline{\mathcal{C}} = \mathcal{C}$ in the finite dimensional case and otherwise $\mathcal{C} \subset \overline{\mathcal{C}}$ in the infinite dimensional case is a suitable distributional extension. That is, the operators satisfy (assuming careful domain definitions) $[\hat{q}, \hat{q}] = [\hat{p}, \hat{p}] = 0$, $[\hat{p}, \hat{q}] = i\hbar \, 1_{\mathcal{H}}$; $\hat{q}^\dagger = \hat{q}$, $\hat{p}^\dagger = \hat{p}$. Here $\overline{\mathcal{C}}$ comes with some topology and μ is a Borel measure on it.

Assuming that also C has a quantization $\hat{C}$ as a positive, self adjoint operator (in field theories this is non trivial due to operator ordering and operator product expansion questions) we construct the operator representation of (2.2) by substituting Poisson brackets by commutators divided by $i\hbar$

$$\hat{z} := \sum_{n=0}^{\infty} \frac{(-i)^n}{n! \, (i\hbar)^n} \{\hat{C}, \hat{q}\}_{(n)} = e^{-\hat{C}/\hbar} \, \hat{q} \, e^{\hat{C}/\hbar} \tag{2.3}$$

This formula explains the dimension restriction on C. The operator $e^{\pm \hat{C}/\hbar}$ is well defined via the spectral theorem. We will refer to $e^{-\hat{C}/\hbar}$ as the *heat kernel* and to $\hat{z}$ as the *annihilation operator*.

The δ distribution δ_{q_0} with support at $q_0 \in \overline{\mathcal{C}}$ on the subset of $\mathcal{H}$ consisting of the continuous functions is defined by

$$\delta_{q_0}[\psi] := \psi(q_0) :=< \delta_{q_0}, \psi >:= \int_{\overline{\mathcal{C}}} d\mu(q) \, \delta_{q_0}(q)\psi(q) \tag{2.4}$$

where $\delta_{q_0}(q)$ is the integral kernel of the unit operator. We define for $z \in \overline{\mathcal{C}}^{\mathbb{C}}$ the *coherent state*

$$\psi_z := [e^{-\hat{C}/\hbar}\delta_{q_0}]_{q_0 \to z} \tag{2.5}$$

It is defined as "heat kernel evolution" followed by analytic continuation. In order that this makes sense, the function $e^{-\hat{C}/\hbar}\delta_{q_0}$ must not only be in $\mathcal{H}$ but also analytic in q_0. This explains the positivity and scaling requirement on C which makes sure that the heat kernel is a damping operator such that at least

for separable $\mathcal{H}$ the function (2.5) is not only normalizable but also analytic. Here we have assumed that the map $\mathcal{C} \to \mathcal{C}^{\mathbb{C}}$; $q \mapsto z$ in (2.2) has an extension to some $\overline{\mathcal{C}}^{\mathbb{C}}$.

The whole point of this construction is that one can easily verify

$$\hat{z}\, \psi_z = z\, \psi_z \tag{2.6}$$

Thus, ψ_z is an eigenfunction of the annihilation operators $\hat{z}$ which explains the notion "coherent state". As is well known, property (2.6) implies that the uncertainty relation for the self adjoint operators

$$\hat{x} := [\hat{z} + \hat{z}^\dagger]/2, \quad \hat{y} := -i[\hat{z} - \hat{z}^\dagger]/2 \tag{2.7}$$

is saturated, that is

$$[<\hat{x}^2>_z - (<\hat{x}>_z)^2]\,[<\hat{y}^2>_z - (<\hat{y}>_z)^2] = \frac{1}{4}\,|<[\hat{x},\hat{y}]>_z| \tag{2.8}$$

where $<\,.\,>_z := <\psi_z,\,.\,\psi_z>/||\psi_z||^2$ denotes the expectation value with respect to ψ_z (notice that ψ_z is in general not automatically normalized). This is a second property commonly attributed to coherent states [35].

Finally, under certain technical assumptions spelled out in [36] the completeness relation

$$1_{\mathcal{H}} = \int_{\overline{\mathcal{C}}} d\mu(q_0)\, \delta_{q_0}\, \delta_{q_0}[.] \tag{2.9}$$

implies that there exists a measure ν on $\overline{\mathcal{C}}^{\mathbb{C}}$ such that

$$1_{\mathcal{H}} = \int_{\overline{\mathcal{C}}^{\mathbb{C}}} d\nu(z)\, \psi_z\, <\psi_z,\,.> \tag{2.10}$$

This concludes the general discussion. The interested reader may verify [22, 24] that the coherent states for Maxwell Theory on Minkowski space result from the complexifier

$$C = \frac{1}{2\kappa^2} \int_{\mathbb{R}^3} d^3x\, \delta_{ab} E^a \sqrt{-\Delta}^{-1} E^b \tag{2.11}$$

where E^a is the Maxwell electric field, Δ is the Laplacian on $\mathbb{R}^3$, κ is the electric charge and $\alpha = \hbar\kappa^2$ is the Feinstruktur constant.

2.2 Complexifiers for Background Independent Gauge Theories

As explained in detail in [37, 38], gauge theories with compact gauge group G provide an almost perfect arena for the general theory summarized in the previous subsection. Let us explain this in some detail:

1. *Classical Phase Space*

   The role of $\mathcal{C}$ is played by some space of smooth connections $\mathcal{A}$ over some $D-$dimensional spatial manifold σ. The role of $\mathcal{M}$ is then simply $T^*\mathcal{A}$. The configuration and momentum coordinates on this phase space then are simply real valued connection one forms $A_a^j(x)$ (potentials) and Lie algebra valued vector densities $E_j^a(x)$ (electric fields) respectively which enjoy the following Poisson brackets

   $$\{A_a^j(x), A_b^k(y)\} = \{E_j^a(x), E_k^b(y)\} = 0, \quad \{E_j^a(x), A_b^k(y)\} = \kappa\, \delta_b^a\, \delta_j^k\, \delta(x,y) \tag{2.12}$$

   Here κ denotes the square of the coupling constant of the gauge theory, $a, b, c, .. = 1, .., D$ denote spatial tensor indices and $j, k, l, .. = 1, .., \dim(G)$ denote Lie algebra indices. We will assume that G is connected, semisimple and take the convention that the internal metric is just δ_{jk}.

8

2. *Distributional Configuration Space*
   Now consider arbitrary, finite piecewise analytic (more precisely semianalytic [15]) graphs embedded in σ which we think of as collections of edges e, that is, piecewise analytic one dimensional paths which intersect at most in their endpoints, called the set $V(\gamma)$ of verticies of γ. Denote by $E(\gamma)$ the set of edges of γ. Given γ consider functions *cylindrical over* γ of the form

   $$f : \; \mathcal{A} \to \mathbb{C}; \; A \mapsto f(A) = f_\gamma(\{A(e)\}_{e \in E(\gamma)}) \tag{2.13}$$

   where $f_\gamma : \; G^{|E(\gamma)|} \to \mathbb{C}$ is a complex valued function on $|E(\gamma|$ copies of G and $A(e)$ denotes the holonomy of A along e. Functions of the form (2.13) form an Abelian * algebra under pointwise operations with the involution given by complex conjugation. We can turn it into an Abelian C^*-algebra, usually called Cyl (cylinder functions) with respect to the sup norm on $\mathcal{A}$ that is

   $$||f|| := \sup_{A \in \mathcal{A}} |f(A)| \tag{2.14}$$

   As is well known [39], Abelian C^*-algebras $\mathfrak{A}$ are isometric isomorphic to another Abelian C^*-algebra which consists of continuous functions on a compact Hausdorff space $\Delta(\mathfrak{A})$, called the spectrum of $\mathfrak{A}$. Denote the spectrum of Cyl by $\overline{\mathcal{A}}$. It has a nice geometrical interpretation as a space of generalized connections in the sense that the holonomy of $A \in \overline{\mathcal{A}}$ satisfies all the usual algebraic relations satisfied by smooth holonomies, that is $A(e \circ e') = A(e)A(e')$ if the end point of e is the beginning point of e' and $A(e^{-1}) = (A(e))^{-1}$, but that smoothness or even continuity is no longer required. The topology on $\overline{\mathcal{A}}$ is the Gel'fand topology which in this case boils down to saying that a net of generalized connections converges when the corresponding net of holonomies for all possible paths converges. See [14, 40, 2] for more details.

3. *Hilbert Space*
   Being a compact Hausdorff space, a natural set of representations of the Poisson$^*-$algebra generated by all the holonomies and all the electric fluxes through co-dimension 1 (piecewise analytic) surfaces S

   $$E_j(S) := \int_S *E_j \tag{2.15}$$

   where $*E_j$ denotes the pseudo $(D-1)$form dual to E_j^a, should be of the form $\mathcal{H} = L_2(\overline{\mathcal{A}}, d\mu)$ where μ is a Borel probability measure. It turns out that all cyclic representations that carry a unitary representation of the diffeomorphism group $\text{Diff}(\sigma)$ are of this form [15] and the corresponding measure is unique and was first discovered in [14]. See e.g. [2] for all details. For our purposes it is enough to know that $\mathcal{H}$ admits a natural orthonormal basis, called spin network functions (SNWF). They are labelled by a graph γ, a collection $\pi = \{\pi_e\}_{e \in E(\gamma)}$ of irreducible, non trivial representations of G and collections $m = \{m_e\}_{e \in E(\gamma)}$, $n = \{n_e\}_{e \in E(\gamma)}$ of integers m_e, $n_e = 1, .., \dim(\pi_e)$ labelling the edges of γ and are explicitly defined by

   $$T_{\gamma,\pi,m,n}(A) := \prod_{e \in E(\gamma)} \sqrt{\dim(\pi_e)} \, [\pi_e(A(e))]_{m_e n_e} \tag{2.16}$$

In order to further apply the general theory of the previous subsection we must provide a complexifier. The complexifier for Maxwell theory displayed in (2.11) is motivated by the fact that the associated annihilation operators are precisely those that enter the Maxwell Hamiltonian. In General Relativity there is no a priori Hamiltonian but there is the Hamiltonian constraint. Hence one might be tempted to choose a complexifier whose associated annihilation operator is related to the Hamiltonian constraint. Unfortunately, the Hamiltonian constraint is, in contrast to Maxwell theory, neither polynomial nor does it have a quadratic piece with respect to which a perturbation scheme can be defined. Hence, the notion of an annihilation

operator defined by the Hamiltonian constraint is ill defined[6]. On the other hand, since we here just want to construct coherent states which approximate well our elementary holonomy and flux operators which are defined on the kinematical Hilbert space (on which the Hamiltonian constraint is not satisfied) in order to verify whether other kinematical operators (i.e. not invariant under the gauge motions generated by the spatial diffeomorphism and Hamiltonian constraints) such as the volume operator have been correctly quantized, the motivation to use the Hamiltonian constraint as a selection criterion for the complexifier is anyway less motivated.

In lack of a better selection criterion, we take here a practical attitude and would like to consider a complexifier which comes close to the Maxwell one (2.11) which obviously satisfies all the requirements of definition 2.1. Since we have applications in General Relativity in mind, we must preserve background independence and therefore the Minkowski background Laplacian entering (2.11) must be replaced by something background metric independent. One possibility is to use a background independent Laplacian which depends on the dynamical 3-metric of q_{ab} which $E_j^a/\sqrt{|\det(E)|}$ is its triad. However, this would lead to a very complicated object with which no practical calculations are possible. In fact, the practical use of coherent states in Maxwell theory rests on the fact that (2.11) is quadratic in the momenta (electric fields) which leads to states which are basically Gaussians in both the position and the momentum representation. This motivates to keep our complexifier quadratic in the momenta as well. Furthermore, we must preserve G invariance. For Abelian gauge theories the electric fields are already gauge invariant but not for non Abelian gauge theories.

Thus a first attempt would be to define as complexifier

$$C \propto \int_\sigma d^3x \, q_{ab} \, E_j^a E_k^b \delta^{jk}/\sqrt{\det(q)} \tag{2.17}$$

where had to replace the background metric δ_{ab} in (2.11) by the dynamical metric and in order to make (2.17) spatially diffeomorphism invariant we have included a density factor $1/\sqrt{\det(q)}$. However, it is easy to see that (2.17) becomes

$$C \propto V = \int_\sigma d^3x \, \sqrt{|\det(E)|} \tag{2.18}$$

the volume functional. While it satisfies the requirements of a complexifier, and admits a quantization as a positive self adjoint operator, its spectral decomposition is not analytically available so that $C = V$ is not practically useful.

Hence, what we need is a gauge invariant, background independent expression, quadratic in the electric fields which preferably is non vanishing everywhere on σ and which can be expressed in terms of (limits of) electric fluxes since only those are well defined in the quantum theory. In [22] it is shown that in non Abelian gauge theories no quadratic complexifier based strictly on fluxes exists that meets all these requirements. The way out is to give up the the requirement that the complexifier is composed out of the fluxes but to allow more general objects than fluxes. There are basically two proposals in the literature. The first [11] replaces fluxes by gauge covariant fluxes. The second [22] replaces the flux by areas. We will review these two proposals separately.

In what follows we assume that as in General Relativity the canonical dimension of E_j^a is cm^0 and that of A_a^j is cm^{-1} so that (2.25) has dimension cm^{D-1}. Since the kinetic term in the canonical action is $\int_\mathbb{R} dt \int_\sigma d^D E_j^a \dot{A}_a^j/\kappa$ it follows that $\hbar\kappa$ has dimension cm^{D-1}.

2.2.1 Gauge Covariant Flux Complexifiers

Given a surface S select a point $p(S) \in S$. Furthermore, for each point $x \in S$ choose a path $\rho_S(x) \subset S$ within S with beginning point $p(S)$ and ending point x. Denote the path system by $\mathcal{P}_S$. The gauge covariant

---

[6]The situation slightly improves when a physical Hamiltonian is available, see [6].

flux of E through S subordinate to the path system $\mathcal{P}_S$ and the edge e_S is defined by

$$E_j(S)\tau_j := \int_S \mathrm{Ad}_{A(\rho_S(x))}((*E)(x)) \tag{2.19}$$

Here $i\tau_j$ are the Pauli matrices, $*E = \frac{1}{2}\epsilon_{abc}dx^a \wedge dx^b\, E_j^c\tau_j$ and Ad denotes the adjoint action of G on its Lie algebra. Obviously, (2.19) transforms in the adjoint representation under gauge transformations at $p(S)$.

Let $\mathcal{S}$ be a collection of surfaces with associated path systems $\mathcal{P}_S$ for each $S \in \mathcal{S}$ and μ a measure on $\mathcal{S}$. Let K be any positive definite, measurable function on $\mathcal{S}$. A gauge covariant flux complexifier (GCFC) is defined by

$$C := \frac{1}{2L^{D-1}\kappa} \int_{\mathcal{S}} d\mu(S)\, K(S)\, [-\frac{1}{2}\mathrm{Tr}(E(S)^2)] \tag{2.20}$$

which is manifestly gauge invariant (one could absorb K, L into μ). Here L is a parameter of dimension of length and we assume both μ, K to be dimensionless.

The mostly studied case is when $D = 3$ and $\mathcal{S} = \mathcal{C}_\in(\mathcal{P})$ is a discrete set of oriented surfaces which coincide with the faces (its sub 2-complex) of a polyhedronal cell partition P of σ. In this case μ is just the counting measure and for convenience one chooses $K = 1$. We will denote the associated complexifier by C_P. In this case the complexified connection is given by

$$Z_a^j(x) = A_a^j(x) - \frac{i}{L^2} \sum_{S \in C_2(P)} \int_S \frac{1}{2}\epsilon_{abc}dy^b \wedge dy^c\, [\mathrm{Tr}(E(S)\, \mathrm{Ad}_{\rho_S(x)}(\tau_j))]\, \delta(x,y) \tag{2.21}$$

Notice that the series involved in Z_a^j terminates at the first term. This is because when computing the second iterated Poisson bracket there is a double sum over surfaces involved but because the paths $\rho_S(x)$ are disjoint from S' for $S' \neq S$ there is no contribution from $S' \neq S$ to $\{C_P, A_a^j(x)\}_{(2)}$. For $S' = S$ there is in principle a contribution but by the regularization [2] the classical flux does not Poisson act on paths lying in its associated surface.

This connection is distributional but fortunately we are only interested in the integral of (2.21) over one dimensional paths e given by

$$iL^2 \int_e dx^a[Z_a^j(x) - A_a^j(x)] = \sum_{S \in C_2(P)} \sum_{x \in S \cap e} \sigma_x(S,e)[\mathrm{Tr}(E(S)\, \mathrm{Ad}_{\rho_S(x)}(\tau_j))] \tag{2.22}$$

where

$$\sigma_z(S,e) = \frac{1}{2} \int_e dx^a\, \epsilon_{abc} \int_S dy^b \wedge dy^c \delta(x,y)\delta_{x,z} \tag{2.23}$$

is the signed intersection number at $z \in e \cap S$ which here we have assumed to be an interior point (otherwise there is an additional factor of $1/2$, in [2]).

2.2.2 Area Compexifier

Let $\mathcal{S}$ be a collection of surfaces, μ a measure on $\mathcal{S}$ and $K(S,S')$ a positive definite integral kernel. An area complexifier is given by the expression

$$C = \frac{1}{a^{D-1}\kappa} \int_{\mathcal{S}} d\mu(S) \int_{\mathcal{S}} d\mu(S)\, K(S,S')\, \mathrm{Ar}(S)\, \mathrm{Ar}(S') \tag{2.24}$$

where a is a parameter of dimension of length. Here $\mathrm{Ar}(S)$ is the gauge invariant "modulus of the electric flux"

$$\mathrm{Ar}(S) := \int_S \sqrt{\mathrm{Tr}([*E]^2)} \tag{2.25}$$

which in General Relativity has the meaning of the *area of S*.

The most studied case arises from a diagonal and constant integral kernel and the following choices of $\mathcal{S}$ and μ respectively.

Definition 2.2.

i.
A stack s in σ is a D-dimensional submanifold with the topology of $\mathbb{R} \times (0,1]^{D-1}$.

ii.
A stack family $S = \{s_\alpha\}$ is a partition of σ into stacks which are mutually disjoint.

iii.
D families of foliations F_I, $I = 1,..,D$ of σ generated by vector fields $\partial/\partial t^I$, $I = 1,..,D$ are said to be linearly independent if the vector fields $\partial/\partial t^I$ are everywhere linearly independent.

iv.
D stack families S^I are said to be linearly independent provided that there exist D linearly independent foliations F_I such that the leaves of the foliation F_I is transverse to every stack in S^I. That is, the intersection $s^I_{\alpha t}$ of any leaf L_{It}, $t \in \mathbb{R}$ of F_I with any stack s^I_α in S^I, called a plaquette, has topology $(0,1]^{D-1}$.

v. The collection of the plaquettes $s^I\alpha t$ is called a parquette at time t within L_{It}.

In general σ will have to be partitioned into pieces that admit D linearly independent foliations each. We construct the complexifier for one such piece below, the complete complexifier is then the sum over the pieces.

The complexifier defined by D linearly independent stack families is now is defined by

$$C := \frac{1}{2\kappa a^{D-1}} \sum_{I=1}^{D} \sum_\alpha \int_\mathbb{R} dt \, [\mathrm{Ar}(p^I_{\alpha t})]^2 \tag{2.26}$$

Here we take the foliation parameter t to be dimensionless, a is a parameter with dimension cm^1 so that $C/\hbar$ is dimensionfree and $p^I_{\alpha t} = s^I_\alpha \cap L_{It}$ denotes the plaquette at time t within the stack s^I_α in direction I. For Abelian gauge theories also the following simpler expression is available

$$C := \frac{1}{2\kappa a^{D-1}} \sum_{I=1}^{D} \sum_\alpha \int_\mathbb{R} dt \, [E_j(p^I_{\alpha t})]^2 \tag{2.27}$$

which uses the gauge invariant flux rather than the areas.

Let us now compute the complexified connections. Notice that due to the fact that each stack is foliated by squares with half open and half closed boundaries, for each $x \in \sigma$ and each direction I there exists a unique stack $s^I_\alpha(x)$ corresponding to a label $\alpha_I(x)$ such that $x \in s^I_\alpha$. Likewise, for each direction I there exists a unique leaf $L_It(x)$ corresponding to a time $t_I(x)$ such that $x \in L_{It}$. Consider the one parameter family of embeddings $X^I_{\alpha t} : [0,1)^{D-1} \to p^I_{\alpha t}$, then there exists a unique $u_I(x)$ such that $x = X^I_{\alpha_I(x)t_I(x)}(u_I(x))$. We now set

$$J_I(x) := |\det(\frac{\partial X^I_{\alpha t}(u)}{\partial(t,u)})|_{\alpha=\alpha_I(x),t=t_I(x),u=u_I(x)}$$

$$n^I_a(x) := \frac{1}{(D-1)!} \epsilon_{ab_1..b_{D-1}} \, \epsilon_{l_1..l_{D-1}} \frac{\partial X^{Ib_1}_{\alpha t}(u)}{\partial u^{l_1}}..\frac{\partial X^{Ib_{D-1}}_{\alpha t}(u)}{\partial u^{l_{D-1}}} \tag{2.28}$$

For the non Abelian complexifier we find

$$Z^j_a(x) = A^j_a(x) - \frac{i}{a^{D-1}} E^b_j(x) \sum_I \frac{n^I_b(x)n^I_a(x)}{J_I(x)} \frac{\mathrm{Ar}(p^I_{\alpha_I(x)t_I(x)})}{\sqrt{[E^c_k(x)n^I_c(x)]^2}} \tag{2.29}$$

while for the Abelian one we obtain

$$Z^j_a(x) = A^j_a(x) - \frac{i}{a^{D-1}} \sum_I \frac{n^I_a(x)}{J_I(x)} E_j(p^I_{\alpha_I(x)t_I(x)}) \tag{2.30}$$

Notice that in both cases the imaginary part of Z^j_a is only quasi local in E^a_j, that is, we can recover E^a_j from Z^j_a only up to the resolution provided by the parquettes.

2.3 Coherent States for Background Independent Gauge Theories

We now come to compute the coherent states. The first step is to write the δ distribution as

$$\delta_{A_0} = \sum_s T_s(A_0) \; <T_s, . > \tag{2.31}$$

where the sum is over all spin network labels $s = (\gamma, \pi, m, n)$. Hence the coherent state is given by

$$\psi_Z = \sum_s T_s(Z) \; <e^{-\hat{C}/\hbar} T_s, . > \tag{2.32}$$

Here $\hat{C}$ is obtained by replacing in (2.19), (2.26) or (2.27) respectively the gauge covariant flux, area or flux functionals by the gauge covariant flux, area or flux operator [11, 8, 41] respectively which are positive, self adjoint operators with pure point spectrum only.

It remains to compute the action of the heat kernel and for this purpose we restrict to the case $D = 3$ of ultimate interest. Again we do this separately for the two types of complexifiers.

2.3.1 Gauge Covariant Flux Coherent States

There is in principle an operator ordering problem involved in the quantization of (2.19), however, the regularization of [2] shows that there is no action of the operator valued distribution $*E(x)$ on a holonomy $A(p)$ if $*E(x)$ is smeared over an infinitesimal surface element of a surface in which the path p lies. Let us introduce the matrices

$$O_{jk}(g) := -\frac{1}{2} \, \mathrm{Tr}(\tau_k \mathrm{Ad}_g(\tau_j)) \tag{2.33}$$

where we have assumed the normalization $\mathrm{Tr}(\tau_j \tau_k) = -2\delta_{jk}$. Since G is compact, we can always embed into a subgroup of some $U(N)$ so that $\overline{\tau_j^T} = -\tau_j$, $\overline{g}^T = g^{-1}$ whence $O_{jk}(g)$ is real valued. Moreover, the obvious identity $O_{jk}(g) = O_{kj}(g^{-1})$ as well as the fact that Ad acts on $\mathrm{Lie}(G)$ whence $Ad_g(\tau_j) = O_{jk}(g)\tau_k$ reveals that

$$O_{jk}(g)O_{jl}(g) = \delta_{kl} \tag{2.34}$$

so that $g \mapsto O_{jk}(g)$ is a subgroup of $O(\dim(G))$.

The known quantization of the non gauge covariant flux [2, 41] together with the above mentioned trivial action on $O_{jk}(A(\rho_S(x)))$ now reveal that

$$\widehat{E_j(S)} T_{\gamma,j,m,n} = i\ell_P^2 \sum_{e \in E(\gamma)} \sum_{x \in S \cap e} \sigma_x(S,e) \, O_{jk}(A(\rho_S(x))) \, \frac{1}{4} X_e^k \, T_{\gamma,j,m,n} \tag{2.35}$$

where X_e^k is the right invariant vector field of G acting on $g = A(e)$, specifically $X_e^k = \mathrm{Tr}(\tau_j g \partial/\partial g^T)$. Here we have assumed that the graph has been adapted to S by suitable subdivisions of edges, such that each edge of γ is either outgoing from an isolated intersection point or completely lies within S or lies completely outside S.

Formula (2.35) can now be plugged into (2.20). Since again there is no action of $widehat E(S)$ on $\rho_S(x)$ we find

$$\widehat{E_j(S)}^2 T_{\gamma,j,m,n} = -\ell_P^4 \sum_{e,e' \in E(\gamma)} \sum_{x \in S \cap e} \sigma_x(S,e) \sum_{y \in S \cap e'} \sigma_y(S,e') \, O_{kl}(A(\rho_S(x)^{-1} \circ \rho_S(y))) \, \frac{1}{16} X_e^k X_{e'}^l \, T_{\gamma,j,m,n} \tag{2.36}$$

The appearance of the matrix $O_{kl}(A(\rho_S(x)^{-1} \circ \rho_S(y)))$ makes the computation of the spectrum of (2.36) rather difficult for a general graph. However, it becomes simple in case that the graph is such that the surface S has only a single isolated intersection point x with the graph. In that case (2.36) becomes

$$\widehat{E_j(S)}^2 T_{\gamma,j,m,n} = -\ell_P^4 [\sum_{e \in E(\gamma)} \sum_{x \in S \cap e} \sigma_x(S,e) \, \frac{1}{4} X_e^j]^2 \, T_{\gamma,j,m,n} \tag{2.37}$$

13

One can now introduce similar as in [41] the vector fields

$$Y_S^{j\pm} = -i \sum_{\sigma_x(e,S)=\pm 1} X_e^j/2, \ Y_S^j = Y_S^{j+} + Y_S^{j-} \tag{2.38}$$

so that we obtain the linear combinations of Casimir operators

$$\widehat{E_j(S)}^2 T_{\gamma,j,m,n} = \frac{\ell_P^4}{4}[2(Y_S^{j+})^2 + 2(Y_S^{j-})^2 - (Y_S^j)^2] \ T_{\gamma,j,m,n} \tag{2.39}$$

A special case arises when x is an interior point of a single edge $e = (e_1)^{-1} \circ e_2$ intersected transversely so that $\sigma_x(S, e_1) = -\sigma_x(S, e_2) = \pm 1$ and thus $T_{\gamma,j,m,n}$ is gauge invariant at x. Then (2.39 further simplifies to

$$\widehat{E_j(S)}^2 T_{\gamma,j,m,n} = \ell_P^4 \ [-iX_e^j/2]^2 \ T_{\gamma,j,m,n} \tag{2.40}$$

For $G = U(1)^3$ or $G = SU(2)$ respectively the eigenvalues of $(-iX_e^j)^2$ are given by $(n_e^j)^2$ and $j_e(j_e + 1)$ respectively. This special case arises for the case of the polyhedronal cell complex complexifier when γ is a graph dual to it, that is, there is precisely one edge e of γ which intersects a given face S and if so transversely.

2.3.2 Area Coherent States

Notice that for each direction I, each graph γ and each stack α the Lebesgue measure of the set of times t such that $p_{\alpha t}^I$ contains a vertex of γ or that $p_{\alpha t}^I$ contains entire segments of edges of γ vanishes. By the properties of the area operator and flux operator, it follows that those points do not contribute to the heat kernel evolution and therefore we may assume without loss of generality that each $p_{\alpha t}^I$ intersects the edges of γ at most transversely in an interior point. Now consider in the non Abelian case for natural numbers $N_e \in \mathbb{N}_0$ the set

$$S_N^{I\alpha\gamma} := \{t \in \mathbb{R}; \ |p_{\alpha t}^I \cap e| = N_e\} \tag{2.41}$$

where we have abbreviated $N := \{N_e\}_{e \in E(\gamma)}$. This is the set of parquettes within stack s_α^I which intersect edge e precisely N_e times transversely. Likewise, consider for the Abelian case for integers $N_e \in \mathbb{Z}$

$$S_N^{I\alpha\gamma} := \{t \in \mathbb{R}; \ \sum_{x \in p_{\alpha t}^I \cap e} \sigma(p_{\alpha,t}^I, e)_p = N_e\} \tag{2.42}$$

where for any surface S intersecting e transversely, the number $\sigma(S, e)_p$ for $p \in S \cap e$ takes the value $+1$ or -1 respectively if the orientations of S and e at p agree or disagree respectively. This is the set of parquettes within stack p_α^I whose signed intersection number with edge e is precisely N_e.

In both cases let

$$l_N^{I\alpha\gamma} := \int_{S_N^{I\alpha}} dt \tag{2.43}$$

be the Lebesgue measure or *length* of those sets. These length functions are needed in order to define a cylindrically consistent family of heat kernels as was first observed in [38]. Then the action of the complexifier on SNWF's is diagonal

$$\frac{\hat{C}}{\hbar} T_s = \lambda_s T_s \tag{2.44}$$

The corresponding eigenvalues are given for $G = SU(2)$ by

$$\lambda_s = \frac{\ell_P^2}{2a^2} \sum_{I,\alpha} \sum_N l_N^{I\alpha\gamma} \ [\sum_{e \in E(\gamma)} N_e \ \sqrt{j_e(j_e + 1)}]^2 \tag{2.45}$$

14

while for $G = U(1)^3$ they are given by

$$\lambda_s = \frac{\ell_P^2}{2a^2} \sum_{I,\alpha} \sum_N l_N^{I\alpha\gamma} \left[\sum_{e \in E(\gamma),j} N_e \, n_e^j \right]^2 \tag{2.46}$$

Here we have used that the irreducible, non trivial representations of $SU(2)$ are given by positive, half integral spin quantum numbers $j_e \neq 0$ while for $U(1)^3$ they are given by triples of integers $n_e^j \neq 0$, $j = 1, 2, 3$. Furthermore, with $\kappa = 8\pi G_{\text{Newton}}$, $\ell_P^2 = \hbar\kappa$ is the Planck area. The ratio $t := \ell_P^2/a^2$ is known as the classicality parameter. Without dynamical input, this is a free parameter for our coherent states that decides up to which scale the fluctuations of operators are negligible.

2.4 Cut – Off Coherent States

Formulae (2.32), (2.36) (2.45) and (2.46) display the coherent states in closed form. Unfortunately, although the eigenvalues of the heat kernel grow quadratically with the representation weight, these states are still not normalizable because the Hilbert space is not separable, or in other words, the SNWF's are labelled by the continuous parameter γ. In view of the uniqueness result when insisting on background independence, the non separability is not avoidable and one must accept it. The observation is that (2.32) defines a well defined distribution on the dense subset of $\mathcal{H}$ consisting of the finite linear span of SNWF's. To extract normalizable information from ψ_Z we introduce the notion of a cut – off state labelled by a graph γ. These are defined by

$$\psi_{Z,\gamma} := \sum_{s;\gamma(s) \subset \gamma} T_s(Z) \; < e^{-\hat{C}/\hbar} T_s, . > \tag{2.47}$$

That is, the sum over all spin networks $s = (\gamma(s), \pi(s), m(s), n(s))$ is truncated or *cut off* to those whose graph entry $\gamma(s)$ is a subgraph of the given γ. The Ansatz is then to use $\psi_{Z,\gamma}$ for suitable γ as a semiclassical state.

Notice that both (2.45) and (2.46) respectively can be rewritten in the form

$$\lambda_s = \frac{t}{2} \sum_{e,e'} l_{e,e'}^{\gamma} \sqrt{j_e(j_e + 1)} \sqrt{j_{e'}(j_{e'} + 1)} \tag{2.48}$$

and

$$\lambda_s = \frac{t}{2} \sum_{e,e'} l_{e,e'}^{\gamma} \, n_e^j \, n_{e'}^j \tag{2.49}$$

where the *edge metric*

$$l_{e,e'}^{\gamma} = \sum_{I,\alpha} \sum_N l_N^{I\alpha\gamma} N_e N_{e'} \tag{2.50}$$

has entered the stage. Such non diagonal edge metrics have already appeared in other background dependent contexts [24, 25]. The edge metric decays quickly off the diagonal because for most edge pairs $e \neq e'$ there is no direction and no stack in that direction intersecting both e, e' which means that $l_N^{I\alpha\gamma} = 0$ for N_e, $N_{e'} \neq 0$ for such edge pairs. It is for this reason that we will be able to actually carry out our calculations.

Using the edge metric, formulas (2.29), (2.30) and (2.45), (2.46) admit an interesting reformulation: The *signed intersection number* between a path e and a surfaces S is defined by (adopting convenient parametrization)

$$\begin{aligned} \sigma(S,e) \; &:= \; \int_e dx^a \int_S dy^b \, dy^c \, \frac{1}{2} \, \epsilon_{abc} \, \delta(x,y) = \int_0^1 dt \int_{[0,1]^2} d^2u \, [\epsilon_{abc} \dot{e}^a(t) \frac{\partial S^b(u)}{\partial u^1} \frac{\partial S^c(u)}{\partial u^2}] \, \delta(e(t), S(u)) \\ &= \; \sum_{x \in S \cap e} \sigma_x(S,e) \end{aligned} \tag{2.51}$$

while the *intersection number* is given by

$$|\sigma|(S, e) :== \int_0^1 dt \int_{[0,1]^2} d^2u \; |\epsilon_{abc} \dot{e}^a(t) \frac{\partial S^b(u)}{\partial u^1} \frac{\partial S^c(u)}{\partial u^2}| \; \delta(e(t), S(u)) \tag{2.52}$$

Both expressions can be regularized in such a way that entire segments of e that lie inside S do not contribute to the integral [41]. Notice that $|\sigma|(e, S) \neq |\sigma(e, S)|$. Then it is not difficult to see that for $SU(2)$

$$l_{e,e'}^\gamma = \sum_{\alpha, I} \int dt \; |\sigma|(e, p_t^{\alpha I}) \; |\sigma|(e', p_t^{\alpha I}) \tag{2.53}$$

while for $U(1)^3$

$$l_{e,e'}^\gamma = \sum_{\alpha, I} \int dt \; \sigma(e, p_t^{\alpha I}) \; \sigma(e', p_t^{\alpha I}) \tag{2.54}$$

To verify (2.53), (2.54) it is easiest to use directly the action of non Abelian area and Abelian flux operators respectively on the corresponding SNWF [41] (with only transverse intersections)

$$\text{Ar}(S)T_{\gamma,j,m,n} = \ell_P^2 \, [\sum_{e \in E(\gamma)} |\sigma|(e, S) \sqrt{j_e(j_e + 1)}] \, T_{\gamma,j,m,n}$$

$$E_j(S)T_{\gamma,n} = \ell_P^2 \, [\sum_{e \in E(\gamma)} \sigma(e, S) \, n_e^j] \, T_{\gamma,n} \tag{2.55}$$

and to plug this formula into the expression for C. An alternative proof is by realizing that in the non Abelian or Abelian case respectively

$$\chi_{S_N^{\alpha I}}(t) = \prod_{e \in E(\gamma)} \delta_{|\sigma|(p_t^{\alpha I}, e), N_e}, \;\; \chi_{S_N^{\alpha I}}(t) = \prod_{e \in E(\gamma)} \delta_{\sigma(p_t^{\alpha I}, e), N_e} \tag{2.56}$$

where χ_S denotes the characteristic function of a set. When plugging (2.56) into (2.50) and solving the Kronecker δ's when carrying out the sum over the integers N, (2.53) and (2.54) respectively result.

From the easily verifiable properties of the (signed) intersection numbers

$$\sigma(e \circ e', S) = \sigma(e, S) + \sigma(e', S), \; \sigma(e^{-1}, S) = -\sigma(e, S); \; |\sigma|(e \circ e', S) = |\sigma|(e, S) + |\sigma|(e', S), \; |\sigma|(e^{-1}, S) = |\sigma|(e, S) \tag{2.57}$$

it follows immediately that

$$l^\gamma(e \circ e', e \circ e') = l^\gamma(e, e) + l^\gamma(e', e') + 2l^\gamma(e, e'), \;\; l^\gamma(e^{-1}, e^{-1}) = l^\gamma(e, e) \tag{2.58}$$

This is precisely the generalization to non diagonal edge metrics of the cylindrical consistency conditions of the complexifier [22, 38]. Notice that for the general area complexifier (2.24) we arrive instead at the edge metrics

$$l_{e,e'}^\gamma = \int_{\mathcal{S}} d\mu(S) \int_{\mathcal{S}} d\mu(S') \; |\sigma|(S, e) \, K(S, S') \, |\sigma|(S', e'), \;\; l_{e,e'}^\gamma = \int_{\mathcal{S}} d\mu(S) \int_{\mathcal{S}} d\mu(S) \; \sigma(S, e) \, K(S, S') \, \sigma(S', e') \tag{2.59}$$

Finally we have for any edge e

$$\int_e dx^a \; ia^2 [Z_a^j - A_a^j](x) = \sum_{I, \alpha} \int dt \; \text{Ar}(p_t^{I\alpha}) \int_0^1 ds \; \frac{(n_c^I E_j^c)(e(s))}{\sqrt{[(n_b^I E_j^b)(e(s))]^2}} \; \int d^2u \; [\dot{e}^a(s) n_a^{\alpha I t}(u) \delta(p_t^{\alpha I}(u), e(s))] \tag{2.60}$$

in the non Abelian case while for the Abelian case

$$\int_e dx^a \; ia^2 [Z_a^j - A_a^j](x) = \sum_{I, \alpha} \int dt \; E_j(p_t^{\alpha I}) \, \sigma(p_t^{\alpha I}, e) \tag{2.61}$$

Interestingly, if E does not vary too much on the scale of a plaquette, then (2.60) actually reduces to (2.61) which is written directly in terms of the signed intersection number and plaquette fluxes. This will be useful later on when we compute expectation values.

16

2.5 Comparison of Gauge Covariant Flux and Area Coherent States

Consider the case that the plaquttes are much smaller than the edges with respect to the three metric to be approximated by the coherent states and that the edges do not wiggle much on the scale of the plaquettes. Then for each I the number of stacks that do not contain a vertex of γ but still intersect γ drastically outnumbers the number of stacks that do contain a vertex. Moreover, among the edge free stacks, the number of stacks that intersect only one edge completely outnumbers the ones that intersect more than one edge. Finally, among those with single edge intersections, the number of stacks that intersect the respective edge once completely outnumbers the ones that do more than once. For this reason, in these cases the expressions (2.45) and (2.46) can be replaced with good approximation by simpler expressions of the form

$$\lambda_s = \frac{\ell_P^2}{2a^2} \sum_{e \in E(\gamma)} l_e^\gamma \, j_e(j_e + 1) \tag{2.62}$$

and

$$\lambda_s = \frac{\ell_P^2}{2a^2} \sum_{e \in E(\gamma)} l_e^\gamma \, [n_e^j]^2 \tag{2.63}$$

respectively where the length function $l_e^\gamma = g_{ee}^\gamma$ solves $l_{eoe'}^\gamma = l_e + l_{e'}$, $l_{e^{-1}} = l_e$ in order that the complexifier has cylindrically consistent projections. This is the form of the heat kernel eigenvalue considered for the states in [38]. As shown in [22], these eigenvalues cannot come from a known classical complexifier so that the complexification map $A \mapsto Z$, without which the Z label of the coherent state has no relation to the phase space point to be approximated, is unknown. When using the complexifier coming from a polyhedronal cell complex, a concrete relation between Z and the phase space can be given for specific graphs, the above eigenvalues arise as we saw in section 2.3.1 and as shown in [22].

Let us also check that the area complexification map Z in (2.29) and (2.30) comes close to the gauge covariant flux one (2.22), at least on certain graphs. Let γ be a graph dual to the cell complex P. Thus, for each edge e there is a unique face S_e which intersects e in an interior point transversely such that $\sigma_{S_e \cap e}(S_e, e) = +1$ and no other face intersects e. Then the gauge covariant flux complexification map at the level of the holonomies is given by [11]

$$A(e) \mapsto g_e(Z) := Z_\gamma(e) = \exp(-i\tau_j E_j(S_e)/L^2) \, A(e) \tag{2.64}$$

For $SU(2)$, $i\tau_j$ are the Pauli matrices while for $U(1)^3$ $i\tau_j = 1$, $j = 1, 2, 3$. In contrast, the area complexification map is given at the level of the holonomies by

$$A(e) \mapsto Z(e) = \mathcal{P} \exp(\int_e Z^j \tau_j) \tag{2.65}$$

where $\mathcal{P}$ denotes path ordering where Z_a^j is given in (2.29) and (2.30) respectively. Now for sufficiently "short" edges we have $Z(e) \approx \exp(\int_e [Z - A]^j \tau_j) A(e)$ to leading order in the edge parameter length. If we assume that E_j^a is slowly varying at the scale of the plaquettes then we have $\mathrm{Ar}(p_{\alpha_I(x)t_I(x)}^I) \approx \sqrt{[E_j^a(x)n_a^I(x)]^2}$ so that (2.29) is approximated by

$$\int_e (Z^j - A^j) \approx -\frac{i}{a^2} \sum_I \int_0^1 \frac{\dot{e}^a(t)n_a^I(e(t))}{J_I(e(t))} \, n_b^I(e(t))E_j^b(e(t)) \tag{2.66}$$

where we have assumed that e is the embedded interval $[0,1]$. Now consider the case that the graph is in fact cubic and that the stack family and the graph are aligned in the following sense:
Suppose that we have an embedding $X : \mathbb{R}^3 \to \sigma; s \mapsto X(s)$. For $\epsilon_{IJK} = 1$ we define $X_t^I(u^1, u^2) := X(s^I = t, s^J = u^1, s^K = u^2)$. This defines linearly independent foliations F^I with leaves $L_{It} = X_t^I(\mathbb{R}^2)$. The corresponding stack families are labelled by $\alpha := (\alpha^1, \alpha^2) \in \mathbb{Z}^2$ and defined by $X_{\alpha t}^I : [0,1)^2 \to$

σ; $X^I_{\alpha t}(u) := X^I_t([\alpha^1 + u^1]l, [\alpha^2 + u^2]l)$ where $l > 0$ is a certain parameter. The edges of the cubic graph are labelled by verticies $v = (v^1, v^2, v^3) \in \mathbb{Z}^3$ and directions I and are defined for $\epsilon_{IJK} = 1$ by $e_{v,I} : [0,1] \to \sigma; e_{vI}(t) := X(s^I = [v^I + t]\delta, s^J = v^J\delta, s^K = v^K\delta)$ where $\delta > 0$ is another parameter.

In this situation, (2.66) can be further simplified to

$$\int_{e_{vI}} (Z^j - A^j) \approx -\frac{i}{a^2}\delta \int_0^1 n^I_b(e_{vI}(t))E^b_j(e_{Iv}(t)) \approx -\frac{i}{a^2}\delta E_j(p^I_v) \tag{2.67}$$

where p^I_v is any plaquette in the stack in I direction intersected by e_{Iv}.

Thus, for cubic graphs, which are the only ones considered so far in semiclassical calculations, we get a close match between (2.64) and (2.67) whenever the cubic graph and the stack families are aligned. However, there is still an important difference:

The parameter area l^2 of the plaquette p^I_v in (2.67) has no a priori relation to the parameter length δ of the edge e_{vI} while the parameter area of the dual face $S_{e_{vI}}$ in (2.64) is of the order δ^2. These considerations reveal that the individual plaquettes of the stacks cannot be interpreted as the faces of a dual graph although roughly $[\delta/l]^2$ of them combine to a face. Hence the states considered in [22] are genuinely different from those in [11].

This will turn out to be important:

We will see that in order to be able to perform practical calculations for $SU(2)$ with off diagonal edge metrics, we need $l \ll \delta$ in order that the edge metric is close to diagonal for generic graphs. It turns out that if we use the same parameter a in the label Z of the state and for the classicality parameter $t = \ell^2_P/a^2$ then the expectation value of the volume turns out to be of the order of $(l/\delta)^3$ too small. Hence, there is a tension between the possibility to perform practical calculations and the correctness of the classical limit. The only analytical calculation possible with $l = \delta$ uses a graph which is aligned with the stacks and thus is necessarily cubic. While the result of that calculation results in the correct classical limit, this calculation is of limited interest because we saw already above that for this case the coherent states of [22] reduce to those of [11] for which we knew already that the classical limit is correct.

However, the purpose of this paper is to test the semiclassical limit for graphs of non cubic topology. This can be done with the states of [11] without limitation. With the states of [22] this is possible if we redefine $Z^j_a \to A^j_a + \frac{a^2}{b^2}(Z^j_a - A^j_a)$ where $b \ll a$. This rescaling is actually not in the spirit of the complexifier programme, but it repairs the semiclassical limit of *all operators* built from the fluxes. It will then turn out that for graphs that satisfy $l/\delta = b/a$ the correct classical limit results for $n = 6$ only. As already mentioned in the introduction, one could rescale the label of the coherent state by a different amount in order to reach the correct semiclassical limit of the volume operator for one and only one $n \neq 6$. However, that would destroy the correct semiclassical limit of other operators such as areas. Hence the rescaling by $(b/a)^2$ is harmless in the sense that it reproduces the semiclassical limit of all operators while $n-$dependent rescaling do not.

Also with respect to the states of [11] the value $n = 6$ is singled out. The fact that the cut off states of [22] have acceptable semiclassical behavior only when the corresponding cut off graph and the label of the coherent state satisfy certain restrictions imposed by the structure that defines the complexifier, in this case the size of the parquettes, is similar to the restrictions imposed on the by the polyhedronal cell complex complexifier [11], namely that the graph be dual to it.

2.6 Justification for Replacing $SU(2)$ by $U(1)^3$

The considerations above have revealed that practically useful cut – off states will be based on graphs which are much coarser than the parquets so that the edge metric is diagonal in very good approximation. We will restrict to such graphs in the calculations that follow and find independent confirmation for that restriction as well in the form of the quality of the semiclassical approximation. Assuming exact diagonality and thus suppressing the corrections coming from off – diagonality which we will show to be small under the made

18

coarseness assumptions, the cut – off states in fact factorizes

$$\psi_{Z,\gamma} = \prod_{e \in E(\gamma)} \psi_{Z,\gamma,e} \tag{2.68}$$

where for $SU(2)$

$$\psi_{Z,\gamma,e}(A) = \sum_{2j=0}^{\infty} (2j+1) \, e^{-\frac{t}{2}l_e^\gamma j(j+1)} \, \chi_j(g_e A(e)^{-1}) \tag{2.69}$$

while for $U(1)^3$

$$\psi_{Z,\gamma,e}(A) = \sum_{n \in \mathbb{Z}^3} e^{-\frac{t}{2}l_e^\gamma \sum_j (n^j)^2} \, \chi_n(g_e A(e)^{-1}) \tag{2.70}$$

Here χ_j and χ_n respectively denotes the character of the $j-$th and $n-$th irreducible representation of $SU(2)$ and $U(1)^3$ respectively.

Under the made assumptions, the edge metrics l_e^γ are identical for both groups because, while $l_N^{I\alpha\gamma}$ is defined for non negative integers N only in the case of $SU(2)$ while for $U(1)^3$ all integers are allowed, for the graphs under consideration for each edge e only either $N_e = +1$ or $N_e = -1$ leads to non vanishing $l_N^{I\alpha\gamma}$ so that these numbers in fact coincide and since we take the diagonal elements of the edge metric (2.50) both signs lead to the same l_e^γ.

Finally, if (A_0, E_0) is the phase space point to be approximated and from which we calculate $Z = Z(A_0, A_0)$ via (2.29) and (2.30) then for $SU(2)$ we have,

$$g_e \approx \exp(-i\tau_j P_0^j(e)) \, \exp(\tau_j \int_e A_0), \quad P_0^j(e) = \frac{1}{b^2} \sum_I \int_0^1 dt \, \frac{\dot{e}^a(t) n_a^I(e(t))}{J_I(e(t))} \, [E_{0j}^b(e(t)) n_b^I(e(t))] \tag{2.71}$$

while for $U(1)^3$ we have

$$g_e = (g_e^j)_{j=1}^3, \quad g_e^j = \exp(-P_0^j(e) + i \int_e A_0^j) \tag{2.72}$$

where as before we have made the approximation

$$\frac{\text{Ar}(p_{\alpha_I(x)t_I(x)}^I)}{\sqrt{[E_k^c(x) n_c^I(x)]^2}} \approx 1 \tag{2.73}$$

which is valid if E_0 is slowly varying at the scale of the plaquettes.

Thus, given $Z = Z(A_0, E_0)$, we have the following abstract situation under the made assumptions:
1.
For each edge e there exist vectors $P_0^j(e), A_0^j(e)$ such that for $SU(2)$ we have $g_e \approx \exp(-i\tau_j P_0^j \tau_j) \exp(\tau_j A_0^j(e)) \in SL(2,\mathbb{C}) = SU(2)^{\mathbb{C}}$ while for $U(1)^3$ we have $g_e = (e^{-P_0^j(e) + i A_0^j(e)})_{j=1}^3 \in (\mathbb{C} - \{0\})^3 = (U(1)^3)^{\mathbb{C}}$. 2.
The coherent states adopt approximately product form $\psi_{Z,\gamma} \approx \prod_{e \in E(\gamma)} \psi_{g_e}$ where

$$\psi_g(h) = \sum_{2j=0}^{\infty} (2j+1) \, e^{-tl_e^\gamma j(j+1)/2} \, \chi_j(gh^{-1}) \tag{2.74}$$

for $h \in SU(2)$ while

$$\psi_g(h) = \sum_{n \in \mathbb{Z}^3} e^{-tl_e^\gamma \sum_{j=1}^3 n_j^2} \, \chi_n(gh^{-1}) \tag{2.75}$$

for $h \in U(1)^3$.

Now, as anticipated in the introduction, using the tools of semiclassical perturbation theory [19] we are able to calculate to expectation value of the volume operator V of LQG with respect to the correct $SU(2)$ coherent states in terms of the expectation value of of a certain operator Q, where $V = \sqrt[4]{Q}$, which we display explicitly in the next section and which is a sixth order polynomial in the right invariant vector fields X_e^j on $SU(2)$ where X_e^j acts on h_e in (2.74). The crucial observation, made in [11], is that if we simply replace the $SU(2)$ right invariant vector fields in Q by $U(1)^3$ right invariant vector fields X_e^j acting on h_e in (2.75) and if we replace the $SU(2)$ coherent states (2.74) by the related $U(1)^3$ coherent states in (2.75), then the remarkable fact is that *the expectation values of polynomials of right invariant vector fields actually coincide to zeroth order in $\hbar$.* By the same argument, this will be also true if we perform the right invariant vector field replacement already at the level of V rather than Q. This observation was also key in the semiclassical analysis of [20, 21].

This feature is maybe not as surprising as it looks at first sight because, after all, the coherent states for both groups are to approximate the same phase space points. The underlying reason is that that the classical phase space of the $SU(2)$ theory (i.e. the range of fields and the symplectic structure) and of the fictive $U(1)^3$ theory actually coincide. It is only when we add the dynamics of the theory as for instance the Gauss constraint that we see a difference. The Gauss law is taken into account in two ways, first by using the appropriate group coherent states, here $SU(2)$ or $U(1)^3$ respectively, which is dictated by the fact that the underlying holonomies take values in the appropriate group. Secondly, one can construct quantum Gauss constraint invariant coherent states [11, 42] by averaging over the gauge group action at the verticies. Denote this group averaging map by η. Then, as shown in [11, 42], we have that $< \eta(\psi_{Z,\gamma}, A\eta(\psi_{Z,\gamma}) >$ and $\psi_{Z,\gamma}, A\psi_{Z,\gamma} >$ agree to zeroth order in $\hbar$ (notice that the Gauss invariant Hilbert space is an honest subspace of the kinematical Hilbert space so that the same inner product can be used) for any Gauss invariant operator A such as the volume operator because the overlap function between coherent states peaked at different phase space points is sharply peaked[7]. This justifies the use of the kinematical states employed in this paper.

To summaries:
Using kinematical $U(1)^3$ coherent states is a convenient approximation for actual $SU(2)$ coherent state expectation value calculations for Gauss invariant operators if one is only interested in the zeroth order in $\hbar$. At non vanishing orders in $\hbar$ there will be differences but we are not interested in them for the purposes of this paper. One may wonder whether the argument made above, namely using kinematical rather than Gauss invariant coherent states also survives when considering the spatial diffeomorphism constraint. This issue, currently under investigation, is more complicated in part because it is not completely obvious which distributional extension of the classical diffeomorphism group one should use [43]. For the purposes of this paper this is of no concern because we are looking at the *local* volume operator which is not spatially diffeomorphism invariant so that expectation value calculations with respect to spatially diffeomorphism invariant coherent states are meaningless. It is the local volume which enters the Hamiltonian and Master constraint and verifying the semiclassical limit of those only makes sense at the kinematical Hilbert space level (one

---

[7]In more detail we have

$$\eta(\psi_{Z,\gamma}) = \int_{G^{|V(\gamma)|}} \prod_{v \in V(\gamma)} d\mu_H(g_v) \, \alpha_g(\psi_{Z,\gamma}) \qquad (2.76)$$

where $\alpha_g(\psi_{Z,\gamma})(A) = \psi_{Z,\gamma}(\alpha_g(A))$ and $[\alpha_g(A)](e) = g(b(e))A(e)g(f(e))^{-1}$ where $b(e)$ and $f(e)$ respectively denote beginning and final point of e respectively. Now due to gauge covariance of the coherent states we have $\alpha_g(\psi_{Z,\gamma}) = \psi_{\alpha_{g^{-1}(Z)},\gamma}$ so that the gauge invariant coherent state expectation value of a gauge invariant operator becomes (using the invariance properties of the Haar measure)

$$\frac{< \eta(\psi_{Z,\gamma}), A\eta(\psi_{Z,\gamma}) >}{||\eta(\psi_{Z,\gamma})||^2} = \frac{\int_{G^{|V(\gamma)|}} \prod_{v \in V(\gamma)} d\mu_H(g_v) \, < \psi_{\alpha_g(Z),\gamma}, A\psi_{Z,\gamma} >}{\int_{G^{|V(\gamma)|}} \prod_{v \in V(\gamma)} d\mu_H(g_v) \, < \psi_{\alpha_g(Z),\gamma}, \psi_{Z,\gamma} >} \qquad (2.77)$$

Now from [11] we know for gauge invariant polynomials A in right invariant vector fields that the peakedness property

$$< \psi_{Z',\gamma}, A\psi_{Z,\gamma} > = \frac{< \psi_{Z,\gamma}, A\psi_{Z,\gamma} >}{||\psi_{Z,\gamma}||^2} \, < \psi_{Z',\gamma}, \psi_{Z,\gamma} > \, [1 + O(\hbar)] \qquad (2.78)$$

holds. Now the claim is immediate.

20

cannot check the correct classical limit of a constraint on its kernel). Once this limit is verified, one has confidence that the physical Hilbert space defined by the Hamiltonian constraint is correct.

3 Regular Simplicial, Cubical and Octahedronal Cell Complexes

In order to perform the calculations in our companion paper [34] for the coherent states of [22], we need the specific embedding of the $n = 4, 6, 8$ valent graph relative to the stack families. This can easiest be done by starting from regular dual simplicial (tetrahedronal), cubical and octahedronal partitions of the three manifold σ. For the coherent states of [11] this section is not needed except that it shows the existence of (regular) polyhedral cell complexes dual to $n = 4, 6, 8$ valent graphs such that all cells of that complex are platonic solid bodies, i.e. tetrahedral, cubes and octahedra respectively.

In fact, it is possible to define such partitions all from refinements of cubical decompositions such as sketched in figure 1. We perform the analysis for each chart $X : \mathbb{R}^3 \to \sigma$ separately and use the Euclidean
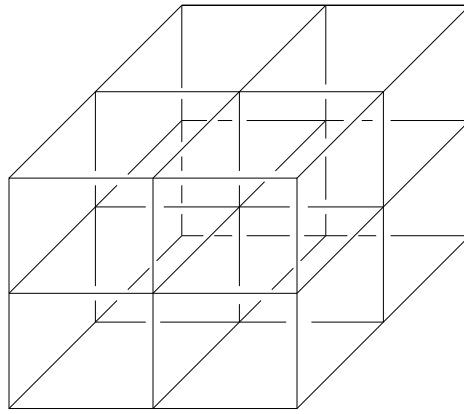
Figure 1: Cubic cell decomposition.

metric on $\mathbb{R}^3$ in the following definitions.

Definition 3.1.
i.
A cubical partition of $\mathbb{R}^3$ is defined by the cubes c_n, $n \in \mathbb{Z}^3$ where

$$c_n = \{s \in \mathbb{R}^3;\ s^I = n^I + t^I,\ I = 1, 2, 3\} \tag{3.1}$$

The boundary faces (squares) of c_n are taken with outward orientation.
ii.
A simplicial partition of $\mathbb{R}^3$ subordinate to a cubical one is defined as follows:
First draw in $c_{(0,0,0)}$ diagonals on the boundary squares such that the diagonals on opposite squares are orthogonal. Specifically, in the face defined by $s^I = 0$; $s^J, s^K \in [0, 1]^2$; $\epsilon_{IJK} = 1$ the diagonal is the line $t \mapsto (s^I = 0, s^J = t, s^K = t)$, $t \in [0, 1]$ while in the face defined by $s^I = 1$; $s^J, s^K \in [0, 1]^2$; $\epsilon_{IJK} = 1$ the diagonal is the line $t \mapsto (s^I = 1, s^J = t, s^K = 1 - t)$, $t \in [0, 1]$.
Now continue this pattern of orthogonal diagonals in opposite faces to the six cubes adjacent to c_0 where common faces have the same diagonal. This also defines the remaining four diagonals in those six cubes by connecting the endpoints of the already present two diagonals.
Finally continue this process for all cubes.
The face diagonals define altogether five tetrahedra that partition each cube. We will take their boundary triangles with outgoing orientation.
iii.

An octahedronal partition of $\mathbb{R}^3$ subordinate to a cubical one is defined as follows:
For each cube draw the unique four space diagonals. Specifically in $c_{(0,0,0)}$ these are the lines $t \mapsto (t,t,t)$, $(t,t,1-t)$, $(t,1-t,t)$, $(1-t,t,t)$; $t \in [0,1]$. These partition each cube into six pyramids with common tip in the barycenter of the cube and with the six faces of the cube as their bases. Now glue two pyramids in adjacent cubes along their common base. Obviously, two glued pyramids define an octahedron which we take with outgoing orientation.

The basic building blocks of the tetrahedronal and octahedronal decompositions are displayed in figures 2, 3 and 4 respectively. When gluing the bases of the pyramids along the faces of the original cubes one
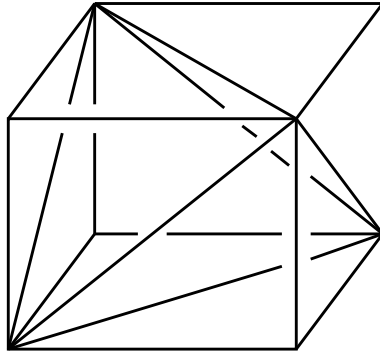
Figure 2: Type A triangulation of a cube.
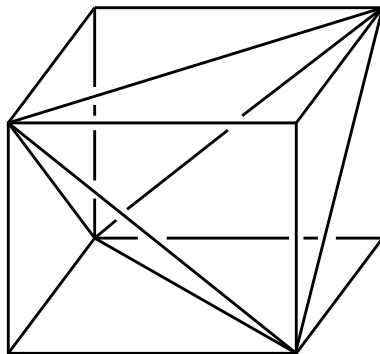
Figure 3: Type B triangulation of a cube.

obtains an octahedronal decomposition as displayed in figure 5. It is maybe not completely obvious that the drawing of the diagonals that are to define the tetrahedra is a consistent and unique prescription. To see this, we use the checkerboard visualization displayed in figurefig7: First draw all plaquettes in the $s^3 = n \in \mathbb{Z}$ layers. Now take the $n = 0$ layer and draw the diagonal for the plaquette in that layer that belongs to $c_{(0,0,0)}$ as prescribed in the definition. Define that plaquette as "black". Now turn the $n = 0$ layer into a checkerboard in the unique way consisting of black and white plaquettes. The other layers $n \neq 0$ are also turned uniquely into checkerboards by asking that checkerboards in adjacent layers are complementary, i.e. if the plaquette (n^1, n^2, n^3) is white (black) then the plaquette $(n^1, n^2, n^3 \pm 1)$ is black (white). Draw diagonals in plaquettes of opposite colour orthogonally to each other. This defines face diagonals in the $s^3 = n$const. layers. These have the property that they form squares in each layer which lie at an angle of $\pi/4$ relative to the plaquettes and which are such that only every second plaquette corner is a vertex of these squares. We will refer to such corners that are verticies as "used". It is easy to see that in adjacent layers, used plaquette corners lie above unused ones. Now draw the remaining face diagonals in the $s^1, s^2 = n =$const. layers by
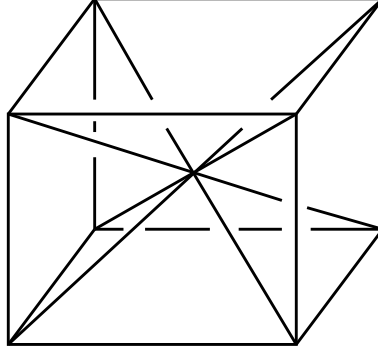
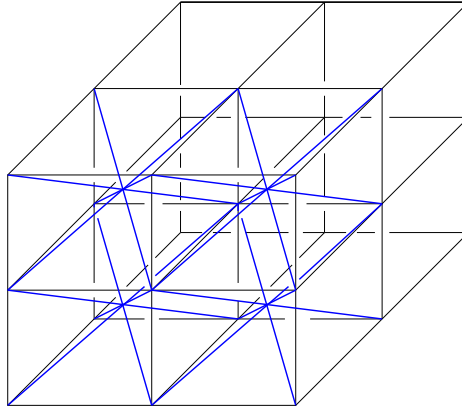Figure 4: Decomposition of a cube into six pyramids.

Figure 5: Octahedronal decomposition.

connecting the used corners in adjacent layers using the appropriate diagonals of the cubes. This results in the triangulation depicted in figure 7. We now define the graphs dual to these particular polyhedronal decompositions.

Definition 3.2.
The graph in $\mathbb{R}^3$ dual to the above simplicial, cubical and octahedronal cell complexes is obtained by connecting the barycentres of adjacent tetrahedra, cubes and octahedra respectively by straight lines through their common triangles, squares and triangles respectively. Here the barycenter of a region $R \subset \mathbb{R}$ is defined as usual by

$$B(R) = \frac{\int_R d^3s \, (s^1, s^2, s^3)}{\int_R d^3s} \tag{3.2}$$

The advantage of the explicit definition of the cell complex is that we can explicitly label the edges and verticies of the dual graph. This is of course only feasible for sufficiently regular graphs, otherwise we run into difficult bookkeeping problems.

1. *Cubical Graph*
   The barycentres of the cubes c_n are evidently the points $v_n := (n^1 + \frac{1}{2}, n^2 + \frac{1}{2}, n^3 + \frac{1}{2})$ which form the verticies of the dual graph. The edges $e_{n,I}$, $I = 1, 2, 3$ which connect the verticies with labels n and $n + b_I$ respectively, where b_I is the standard unit vector $(b_I)^J = \delta_I^J$, have the explicit parametrization $e_{n,I}(t) = v_n + tb_I$, $t \in [0, 1]$. The other three edges adjacent to v_n are ingoing and are given by $e_{n-b_I,I}$. These edges form the 1 skeleton of another cubical cell complex which is just shifted by the vector $(\frac{1}{2}, \frac{1}{2}, \frac{1}{2})$ from the original one.
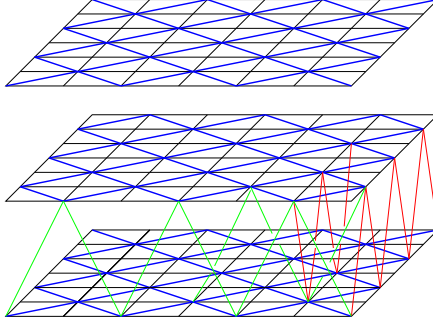
23
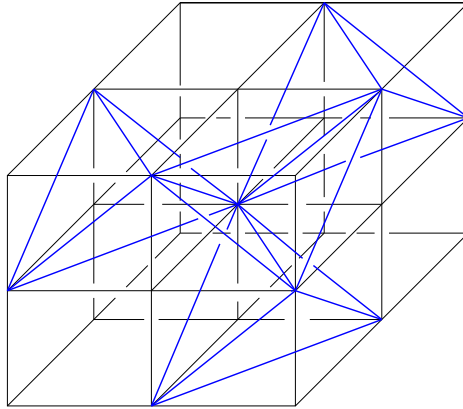
Figure 6: Checkerboard visualization of the triangulation.

Figure 7: Triangulation.

2. *Tetrahedronal graph*

The tetrahedronal graph is the most complicated one because there are two different types of simplicial decompositions of a cube into five tetrahedra. Type A. corresponds to the case that the verticies of the internal tetrahedron within a standard unit cube are given by $(0,0,0)$, $(1,1,0)$, $(1,0,1)$, $(0,1,1)$ while type B. has verticies at $(1,0,0)$, $(0,1,0)$, $(0,0,1)$, $(1,1,1)$. These types alternate in adjacent cubes as we move in any of the three coordinate directions. Hence, by defining the cube c_0 to be of type A., the triangulation is completely completely specified. Indeed, the type of c_n is A. if $n^1 + n^2 + n^3$ is even and of type B. otherwise.

To determine the dual graph, we first discuss the barycentres of the tetrahedra for the two types separately for a standard unit cube as well as the edges of the dual graph that lie within it. The verticies of and the edges in c_n follow then by translation by $n = n^I b_I$. Notice that a tetrahedron T based at v and spanned by vectors e_I, that is, $T = \{v + t^I e_I; \ 0 \leq t^I \leq 1; \ t^1 + t^2 + t^3 \leq 1\}$, has barycenter at $B(T) = v + \frac{1}{4}(e_1 + e_2 + 3_3)$.

A. *Type A.*

The barycenter of the interior tetrahedron coincides with the barycenter $v_0 := \frac{1}{2}(1,1,1)$ of the cube. The barycentres of the remaining four exterior tetrahedra based at verticies $(1,0,0)$, $(0,1,0)$, $(0,0,1)$, $(1,1,1)$ respectively are at $v_1^A := \frac{1}{4}(3,1,1)$, $v_2^A = \frac{1}{4}(1,3,1)$, $v_3^A = \frac{1}{4}(1,1,3)$, $v_4^A = \frac{1}{4}(3,3,3)$ respectively. Accordingly, the dual edges within the cube are $e_\alpha^A = v_\alpha^A - v_0$, $\alpha = 1,2,3,4$.

B. *Type B.*

The barycenter of the interior tetrahedron coincides with the barycenter $v_0 := \frac{1}{2}(1,1,1)$ of the

24

cube. The barycentres of the remaining four exterior tetrahedra based at verticies $(0,0,0)$, $(1,1,0)$, $(1,0,1)$, $(0,$
respectively are at $v_4^B := \frac{1}{4}(1,1,1)$, $v_3^B = \frac{1}{4}(3,3,1)$, $v_2^B = \frac{1}{4}(3,1,3)$, $v_1^B = \frac{1}{4}(1,3,3)$ respectively.
Accordingly, the dual edges within the cube are $e_\alpha^B = v_\alpha^B - v_0$, $\alpha = 1,2,3,4$.

It remains to describe the dual edges that result from gluing the faces of the exterior tetrahedra of adjacent cubes. But this is simple because each of the exterior tetrahedra within a cube has three triangles as faces which lie in the three coordinate planes, hence the gluing is between those triangles which result from drawing the respective face diagonal within a boundary square of a cube. Hence, each cube has twelve edges perpendicular to the twelve boundary triangles of the exterior tetrahedra which are adjacent to the four barycentres of those exterior tetrahedra. Altogether we can identify six possible gluings, namely either going from type A. to type B. when moving along the positive I direction and gluing along the s^I =const. plane or going from type B. to type A. when moving along the positive I direction and gluing along the s^I =const. plane. As one may check, the type A. to type B. gluing in I direction corresponds to two dual edges running from v_I^A to a v_4^B and from v_4^A to v_I^B types of verticies respectively. Likewise, the type B. to type A. gluing in I direction corresponds to two dual edges running from v_J^A to v_K^B and from v_K^A to v_J^B types of verticies respectively where ϵ_{IJK}. In all cases, these I direction edges have coordinate length $\frac{1}{2}$ as one may easily calculate.

Altogether, we can now easily describe the dual lattice as follows:
The verticies are labelled $v_{n,\alpha}$, $\alpha = 0,1,2,3,4$ with $v_{n,0} = n + v_0$ and $v_{n,\alpha} = n + v_\alpha^A$, $\alpha = 1,2,3,4$ if $n^1 + n^2 + n^3$ is even while $v_{n,\alpha} = n + B_\alpha^A$, $\alpha = 1,2,3,4$ if $n^1 + n^2 + n^3$ is odd. The edges are labelled by $e_{n,\alpha}$, $\alpha = 1,2,3,4$ and $e_{n,I,j}$, $I = 1,2,3$, $j = 1,2$ where $e_{n,\alpha}(t) = n + v_0 + t(v_\alpha^A - v_0$ if $n^1 + n^2 + n^3$ is even, $e_{n,\alpha}(t) = n + v_0 + t(v_\alpha^B - v_0)$ if $n^1 + n^2 + n^3$ is odd, $e_{n,I,1}(t) = n + v_I^A + \frac{t}{2}b_I$ and $e_{n,I,2}(t) = n + v_4^A + \frac{t}{2}b_I$ if $n^1 + n^2 + n^3$ is even and finally $e_{n,I,1}(t) = n + v_J^A + \frac{t}{2}b_I$ and $e_{n,I,2}(t) = n + v_K^A + \frac{t}{2}b_I$ if $n^1 + n^2 + n^3$ is odd where $\epsilon_{IJK} = 1$.

3. *Octahedronal Graph*
   Each cube contains six pyramids or halves of the octahedra. Therefore the barycenter of an octahedron coincides with the barycenter of the common boundary face of the two cubes that contain it. It follows that the octahedra may be labelled by $o_{n,I}$ corresponding to the verticies $v_{n,I} = n + \frac{1}{2}b_J + \frac{1}{2}b_K$; $\epsilon_{IJK} = 1$ which define its barycenter. Such an octahedron has the property that it has a common base of two pyramid halves which lies in the s^I =const. plane. For the vertex $v_{n,I}$ we define four edges $e_{n,I,J,\sigma}$, $J \neq I$; $\sigma = \pm$ outgoing from it through the explicit parametrization $e_{n,I,j}(t) := v_{n,I} + \frac{t}{2}(b_I + \sigma b_J)$ which connects the verticies $v_{n,I}$ and $v_{n+\frac{1}{2}(1+\sigma)b_J,J}$. Notice that these edges lie in the (I,J) or (I,K) plane but there are no edges in the (J,K) plane adjacent to $v_{n,I}$. The other four edges adjacent to $v_{n,I}$ have ingoing orientation.

   As an aside, notice that the 1-skeleton of an octahedral cell complex as defined above is an eight valent graph after removing the edges of the original cubes.

The basic building blocks of the dual graphs are displayed in figures 8, 9, 10 and 11 respectively. The connection of the tetrahedronal lattice with the diamond lattice is as follows:
For each cube of type A. or B. respectively, keep the interior tetrahedron. Now move the barycentres of the remaining exterior tetrahedra into that corner of the cube which is also a corner of the tetrahedron under consideration. In this process, the edges dual to the faces of the interior tetrahedron become halves of the spatial diagonals of the cube. Finally drop all the other edges which were running between the barycentres of the exterior tetrahedra. The result is a diamond lattice. Its basic building blocks are depicted in figures 12 and 13 respectively. It is also four valent, however, it does not have a piecewise linear polyhedronal complex dual to it (i.e. whose faces (which are subsets of linear planes) are in one to one correspondence with the edges). It does have a cell complex dual to it if one gives up piecewise linearity by suitably rounding off corners but that is inconvenient to describe analytically. On the other hand, the natural polyhedronal complex consisting of the interior tetrahedra of the original cubes with the cubes deleted consists of those tetrahedra as well octahedra which surround half of the corners of the original cubes. Only half of the
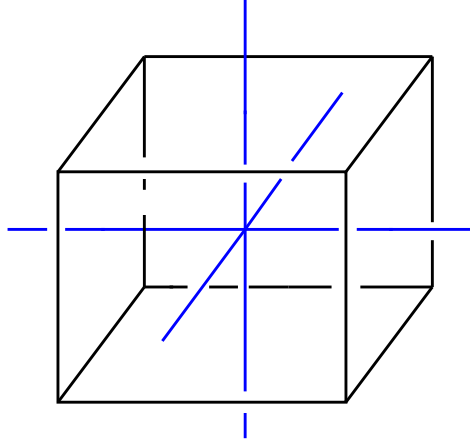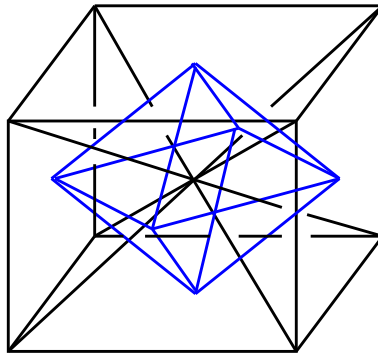
Figure 8: Cube and dual six vallent graph.

Figure 9: Octahedron and dual eight valent graph.

triangle faces of those octahedra are penetrated by the edges of the diamond lattice. The building of this semi dual polyhedronal cell complex consisting of tetrahedra and octahedra respectively is visualized in figures 14, 15, 16, 17 and 18 respectively. In order to achieve the desired duality, one has to fill in the original cubes again which then triangulate those octahedra into eight tetrahedra. This then results in the additional verticies and edges that we described and depicted in figures 10 and 11.

4 Volume Operator Expectation Values for Dual Cell Complex Coherent States

In this section we compute the expectation value of the volume operator with respect to the dual cell complex coherent states of [11]. This section is subdivided into two parts. In the first we review the definition of the Volume Operator. In the second, we perform the actual calculation. In order to carry it out explicitly, we have to specify the graph and the dual cell complex. Here we focus our attention on arbitrary graphs with the following properties: 1. All verticies have constant valence $n = 4, 6, 8$ and 2. the dual cell complex consists only of tetrahedra, cubes and octahedra respectively. Such graphs and dual cell complexes exist as we showed explicitly in section 3. This is all we need for the purposes of this section, more specifics about the graph and the complex are not needed.
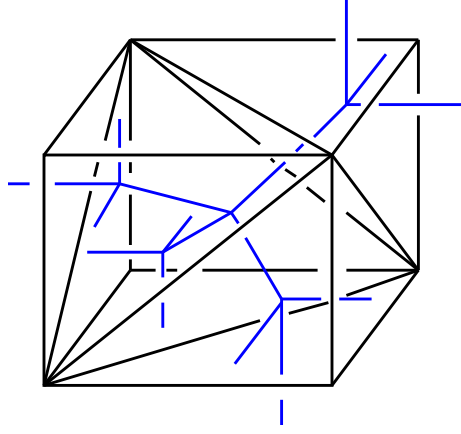
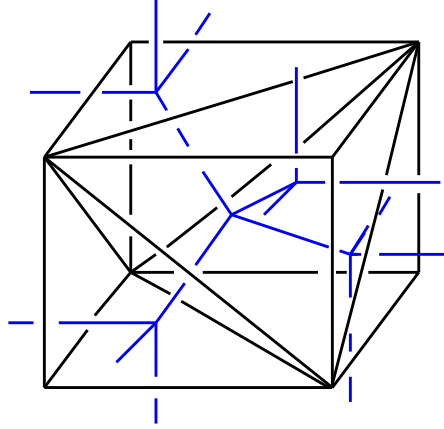Figure 10: Type A triangulation of a cube and dual four valent graph.

Figure 11: Type B triangulation of a cube and dual four valent graph.

4.1   Review of the Volume Operator

The classical expression for the volume of a region R of a semianalytical three dimensional manifold σ is:

$$V_R := \int_R d^3x \ \sqrt{\det(q)} = \int_R d^3x \ \sqrt{|\det E|} \qquad (4.1)$$

where q_{ab} is the three metric. The version of the volume operator [9] consistent with the triad quantization [10] that enters the quantum dynamics [4] has cylindrically consistent projections $\widehat{V}_{R,\gamma}$ given by

$$\hat{V}_R = \sum_{v \in V(\gamma) \cap R} \hat{V}_{\gamma,v} \qquad (4.2)$$

where

$$\hat{V}_{\gamma,v} = \ell_P^3 \sqrt{\left| \frac{1}{8} \sum_{e_I,e_J,e_K,I \leq J \leq K \leq N | v \in e_I \cap e_J \cap e_K} \epsilon^{ijk} \epsilon(e_I, e_J, e_K) X_i^{e_I(v)} X_j^{e_J(v)} X_k^{e_I(v)} \right|} \qquad (4.3)$$

Here N denotes the valence of the vertex, $\ell_P^2 = \hbar\kappa$ is the Planck area, $X_i^{e_I(v)} = \mathrm{Tr}([\tau_i h_I]^T \partial/\partial h_I)$ are right invariant vector on $SU(2)$ acting on the holonomy $h_I := A(e_I)$ ($i\tau_j = \sigma_j$ are the Pauli matrices) and
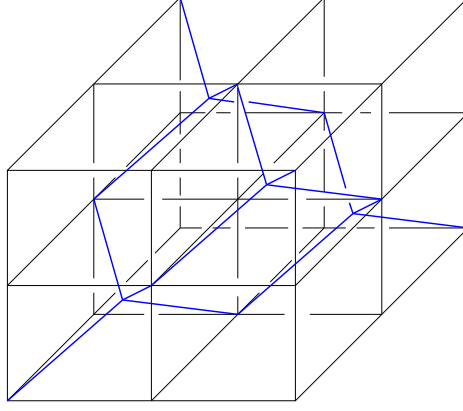
27

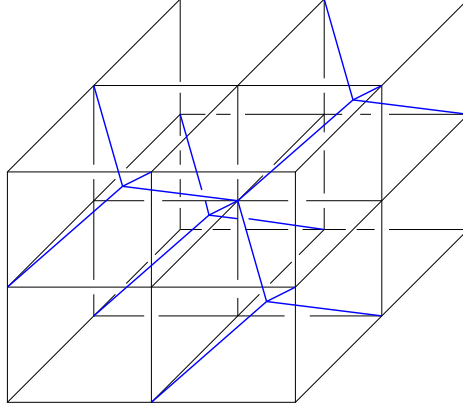Figure 12: Type A diamond cell with occupied lower, left front cube.

Figure 13: Type B diamond cell with unoccupied lower, left front cube.

$\epsilon(e_I, e_J, e_K)$ is called the orientation function which is defined as follows:

$$\epsilon(e_I, e_J, e_K) = \begin{cases} 1, \text{iff } \dot{e}_I, \dot{e}_J, \dot{e}_K \text{are linearly independent at v and positively oriented} \\ -1, \text{iff } \dot{e}_I, \dot{e}_J, \dot{e}_K \text{are linearly independent at v and negatively oriented} \\ 0, \text{iff } \dot{e}_I, \dot{e}_J, \dot{e}_K \text{are linearly dependent at v} \end{cases} \qquad (4.4)$$

Here we take the convention that the edges at v have been taken with outgoing orientation, hence if in γ the orientation of an edge e adjacent to v is actually ingoing, just apply the above expression to $\psi'(.., h_e^{-1}, ...) := \psi(.., h_e, ..)$.

From (4.2), we deduce that the volume operator is a sum of contributions, one for each vertex. Therefore, in the expectation value calculations that follow it will be sufficient to calculate the expectation values for each $\hat{V}_{\gamma,v}$ separately and then to add the contributions. Notice that each of these contributions is of the form $V_{\gamma,v} = \sqrt[4]{Q_{\gamma,v}}$ where $Q_{\gamma,v}$ is minus the square of the expression appearing between the modulus labels $|..|$ in (3.2) and therefore is a sixth order polynomial in the $SU(2)$ right invariant vector fields.

We will now proceed to calculate the general expression for the expectation value of the volume operator for an $n = 4, 6, 8$ valent graph.
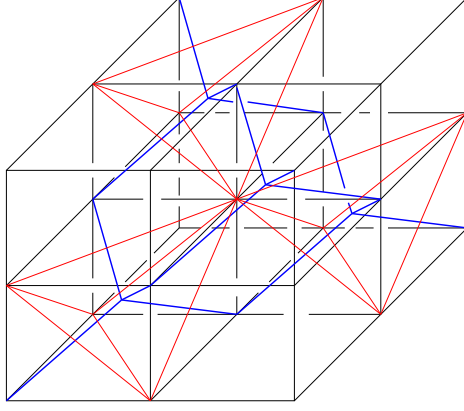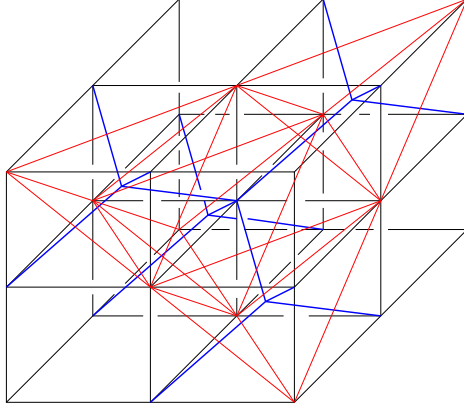
Figure 14: Dual diamond cell of type A.

Figure 15: Dual diamond cell of type B.

4.2 Expectation Values

We can actually perform a full $SU(2)$ calculation as follows:

The coherent states are explicitly given by [11]

$$\psi_{Z,\gamma} = \prod_{e \in E(\gamma)} \psi_{Z,e}, \ \ \psi_{Z,e}(A) = \sum_{2j=0}^{\infty} e^{-tj(j+1)/2} \ \chi_j(g_e(Z)A(e)^{-1}) \tag{4.5}$$

where $t = \ell_P^2/L^2$ and $g_e(Z)$ is given by (2.64). The volume operator expectation value is given by

$$< V(R) >_{Z,\gamma} = \sum_{v \in V(\gamma) \cap R} < V_{\gamma,v} >_{Z,\gamma} \tag{4.6}$$

Notice that due to the product form (4.5), the expectation value $< V_{\gamma,v} >_{Z,\gamma}$ only involves the edges adjacent to v. Now as we saw in the previous section we have $V_{\gamma,v} = \sqrt[4]{Q_{\gamma,v}}$. By the arguments presented in the introduction, the zeroth order in $\hbar$ of $< V_{\gamma,v} >_{Z,\gamma}$ is given by $\sqrt[4]{< Q_{\gamma,v} >_{Z,\gamma}}$. Since $Q_{\gamma,v}$ is a polynomial in right invariant vector fields, the results of [11] reveal that to zeroth order in $\hbar$ the expectation value of any polynomial in the right invariant vector fields $i\ell_P^2 X_e^j$ is simply obtained by replacing it by $E_j(S_e)$ which is given in (2.19).
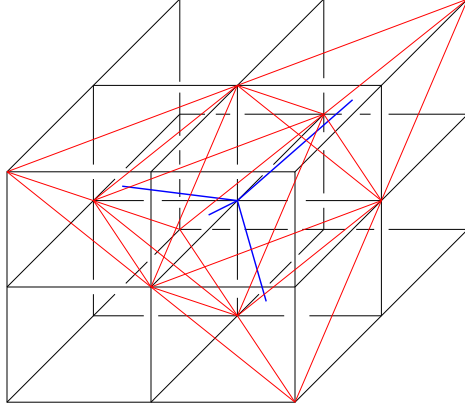
29

Figure 16: Dual diamond cell of type B with only the central four valent vertex left.
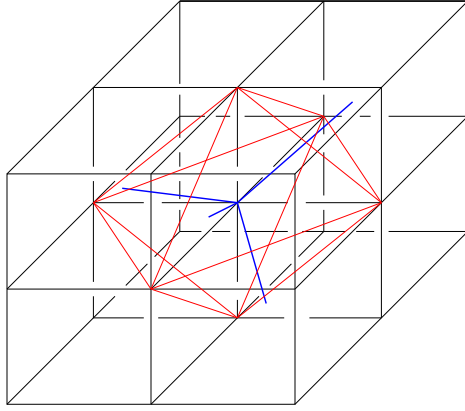

Figure 17: Dual diamond cell of type B with only the central four valent vertex left and keeping only the faces adjacent to the vertex.

It follows that to zeroth order in $\hbar$ we have $< Q_{\gamma,v} >_{Z,\gamma} = [P_{\gamma,v}(E)]^2$ where

$$P_{\gamma,v}(E) = \frac{1}{48} \sum_{e \cap e' \cap e''} \epsilon_{e,e',e''}) \, \epsilon^{jkl} \, E_j(S_e) \, E_k(S_{e'}) \, E_l(S_{e''}) \tag{4.7}$$

Notice that for sufficiently fine graphs, we can drop the holonomies along the paths $\rho_e(x)$ involved in the definition of $E_j(S_e)$ as we approach the continuum. It is then clear that the correct expectation value of the volume operator is reached provided that (4.7) approximates the volume, as specified by E_j^a, of the cell of the polyhedronal complex which is bounded by the faces S_e involved in (4.7).

To do this, we use the fact that for sufficiently fine graphs a polyhedron P in σ dual to a vertex of the graph lies in the domain of a chart Y so that P is the image under Y of a standard polyhedron P_0 in $\mathbb{R}^3$. Introducing

$$n_a^I(s) = \frac{1}{2} \, \epsilon_{abc} \, \epsilon^{IJK} \, \frac{\partial Y^b(s)}{\partial s^J} \, \frac{\partial Y^c(s)}{\partial s^K} \tag{4.8}$$

we immediately find with $P = Y(P_0)$

$$\text{Vol}(P) = \int_P d^3x \, \sqrt{|\det(E)(x)|} = \int_{P_0} d^3s \, \sqrt{|\det(\tilde{E}(s)|} \tag{4.9}$$

where

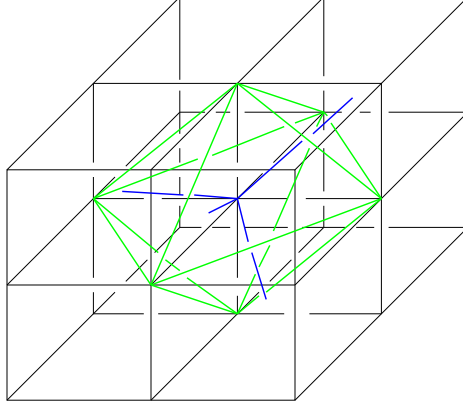$$\tilde{E}_j^I(s) = E_j^a(Y(s)) \, n_a^I(s) \tag{4.10}$$

30

Figure 18: Dual diamond cell of type B with only the central four valent vertex left and keeping only the faces adjacent to the vertex, highlighting its octahedronal cell structure.

Now for sufficiently fine graphs (4.10) is approximately constant over P_0 so that

$$\text{Vol}(P) \approx \sqrt{|\det(\tilde{E}(s)|_{Y(s)=v}} \ \text{Vol}_0(P_0) \tag{4.11}$$

where

$$\text{Vol}_0(P_0) = \int_{P_0} d^3s \tag{4.12}$$

is the volume of the standard polyhedron with respect to the Euclidean metric on $\mathbb{R}^3$.

The idea behind this rewriting is that the fluxes $E_j(S_e)$ can be approximated by specific linear combinations of the $[\tilde{E}_j^I(s)]_{Y(s)=v}$ so that a direct comparison between (4.7) and (4.12) is possible. This is because a boundary face S is also the image under Y of a standard face S^0 in $\mathbb{R}^3$ so that (dropping the holonomies along the $\rho_e(x)$ as explained)

$$E_j(S) = \int_S \frac{1}{2} \epsilon_{abc} \, dx^b \wedge dx^c \, E_j^a(x) = \int_{S^0} \frac{1}{2} \epsilon_{IJK} \, ds^J \wedge ds^K \, \tilde{E}_j^I(s) \approx [\tilde{E}_j^I(s)]_{Y(s)=v} \, \text{F}^I(S^0) \tag{4.13}$$

where

$$\text{F}_I(S^0) = \int_{S^0} \frac{1}{2} \epsilon_{IJK} \, ds^J \wedge ds^K \tag{4.14}$$

is the I component of the Euclidean flux through S_0. Thus, plugging (4.14) into (4.7) we find

$$|P_{\gamma,v}(E)|^{1/2} \approx \sqrt{|\det(\tilde{E}(s))}_{Y(s)=v} \, \text{Vol}_0(v) \tag{4.15}$$

where

$$\text{Vol}_0(v) = \sqrt{|\frac{1}{48} \sum_{e \cap e' \cap e''} \epsilon_{e,e',e''}) \, \epsilon^{IJK} \, F_I(S_e^0) \, F_J(S_{e'}^0) \, F_K(S_{e''}^0)|} \tag{4.16}$$

It remains to compare (4.12) and (4.16). All of this still holds for general graphs. We now specify to purely $n = 4, 6, 8$ valent graphs with the above specified properties in order to test the correctness of the expectation value for specific, simple situations. Thus we know that for each vertex v the faces S_e dual to the edges e adjacent to v form the surface a tetrahedron, cube and octahedron respectively. Thus we just have to compare (4.7) with the volume of such platonic bodies as measured by E_j^a. We will discuss the three cases separately.

4.2.1 Tetrahedron

A standard tetrahedron is the subset

$$T_0 = \{s \in \mathbb{R}^3 : 0 \le s^I \le 1;\ I = 1, 2, 3,\ s^1 + s^2 + s^3 \le 1\} \tag{4.17}$$

It has four boundary triangles given by

$$
\begin{aligned}
t_I^0 &= \{s \in \mathbb{R}^3 : s^I = 0,\ 0 \le s^J, s^K \le 1,\ s^J + s^K \le 1;\ \epsilon_{IJK} = 1\} \\
t_4^0 &= \{s \in \mathbb{R}^3 : 0 \le s^I \le 1;\ I = 1, 2, 3,\ s^1 + s^2 + s^3 = 1\}
\end{aligned} \tag{4.18}
$$

We easily compute

$$\mathrm{Vol}_0(T_0) = \frac{1}{6} \tag{4.19}$$

while (remembering that the surfaces carry outward orientation if the edges are outgoing from v)

$$F_I(t_J^0) = \frac{1}{2}\delta_{IJ},\ F_I(t_4^0) = -\frac{1}{2} \tag{4.20}$$

Let us label the edges adjacent to v by $e_1, .., e_4$ where e_α is dual to $Y(t_j^0)$, $j = 1, 2, 3, 4$. Then

$$
\begin{aligned}
\mathrm{Vol}_0(v) &= = \sqrt{\left|\frac{1}{8} \sum_{1 \le j < k < l \le 4} \epsilon_{e_j, e_k, e_l})\ \epsilon^{IJK}\ F_I(t_j^0)\ F_J(t_k^0)\ F_K(t_l^0)\right|} \\
&= \frac{1}{8}\sqrt{|\epsilon(e_1, e_2, e_3) - \epsilon(e_1, e_2, e_4) - \epsilon(e_1, e_3, e_4) - \epsilon(e_2, e_3, e_3)|}
\end{aligned} \tag{4.21}
$$

which still depends on the sign factors. Hence the expectation value takes values in the range $0, \frac{1}{8}, \frac{\sqrt{2}}{8}, \frac{\sqrt{3}}{8}, \frac{1}{4}$ none of which coincides with $\frac{1}{6}$. For the explicit four valent graph that we constructed in section (3) each triple among the four edges has linearly independent tangents at v and the expectation value is given by $\frac{\sqrt{2}}{8} > \frac{1}{6}$ which is too large.

4.2.2 Cube

A standard cube is the subset

$$C_0 = \{s \in \mathbb{R}^3 : 0 \le s^I \le 1;\ I = 1, 2, 3\} \tag{4.22}$$

It has six boundary squares given by

$$
\begin{aligned}
s_{I+}^0 &= \{s \in \mathbb{R}^3 : s^I = 1,\ 0 \le s^J, s^K \le 1;\ \epsilon_{IJK} = 1\} \\
s_{I-}^0 &= \{s \in \mathbb{R}^3 : s^I = 0,\ 0 \le s^J, s^K \le 1;\ \epsilon_{IJK} = 1\}
\end{aligned} \tag{4.23}
$$

We easily compute

$$\mathrm{Vol}_0(T_0) = 1 \tag{4.24}$$

while (remembering that the surfaces carry outward orientation if the edges are outgoing from v)

$$F_I(s_{J\sigma}^0) = \sigma\delta_{IJ} \tag{4.25}$$

with $\sigma = \pm$.

Let us label the edge dual to $Y(s_{I\sigma}^0)$ by $e_{I\sigma}$. Then the expectation value becomes

$$\mathrm{Vol}(v) = \sqrt{\left|\frac{1}{48} \sum_{I,J,K;\sigma_1,\sigma_2,\sigma_3} \epsilon(e_{I\sigma 1}, e_{J\sigma 2}, e_{K\sigma 3})\ \sigma_1\sigma_2\sigma_3\ \epsilon_{IJK}\right|} \tag{4.26}$$

which again depends on the precise embedding of the graph. For an actual cubical graph constructed in section 3, the edges e_{I+}, e_{I-} are analytic continuations of each other so that the orientation factor vanishes if two or more edges carry the same direction label I. Otherwise there are more contributions. Which orientation factors are allowed has been analyzed in detail in [18]. In the case of the actual cubical graph we have $\epsilon(e_{I\sigma 1}, e_{J\sigma 2}, e_{K\sigma 3}) = \sigma_1 \sigma_2 \sigma_3 \epsilon_{IJK}$ so that (4.26) becomes

$$\text{Vol}(v) = \sqrt{\left| \frac{1}{6} \sum_{I,J,K} \epsilon^2_{IJK} \right|} = 1 \tag{4.27}$$

which coincides with (4.24).

4.2.3   Octahedron

A standard octahedron is the subset

$$O_0 = \{s \in \mathbb{R}^3 : |s^3| \leq \frac{1}{2}, |s^1|, |s^2| \leq \frac{1}{2} - |s^3|\} \tag{4.28}$$

It has eight boundary triangles given by

$$t^0_{I\sigma\sigma'} = \{s \in \mathbb{R}^2 : 0 \leq \sigma' s^3 \leq \frac{1}{2}, s^I = \sigma(\frac{1}{2} - |s^3|), |s^J| \leq \frac{1}{2} - |s^3|\} \tag{4.29}$$

where $I, J = 1, 2$; $I \neq J$; $\sigma, \sigma_3 = \pm$.
   We easily compute

$$\text{Vol}_0(O_0) = \frac{1}{3} \tag{4.30}$$

while (remembering that the surfaces carry outward orientation if the edges are outgoing from v)

$$F_I(t^0_{J\sigma\sigma'}) = \frac{1}{4}[\sigma \delta_{IJ} + \sigma' \delta_{I3}] \tag{4.31}$$

Labelling the edge dual to $Y(t^0_{I\sigma\sigma_3})$ by $e_{I\sigma\sigma_3}$ we find for the expectation value

$$\text{Vol}_0(v) = \sqrt{\left| \frac{1}{48 \cdot 64} \sum_{\substack{I_1, I_2, I_3 = 1,2 \\ \sigma_1, \sigma_2, \sigma_3, \sigma'_1, \sigma'_2, \sigma'_3 = \pm}} \epsilon(e_{I_1 \sigma_1 \sigma'_1}, e_{I_2 \sigma_2 \sigma'_2}, e_{I_3 \sigma_3 \sigma'_3}) [\sigma_1 \sigma_2 \sigma'_3 \epsilon^{I_1 I_2} + \sigma_1 \sigma'_2 \sigma'_3 \epsilon^{I_3 I_1} + \sigma'_1 \sigma_2 \sigma_3 \epsilon^{I_2 I_3}] \right|}$$
$$\tag{4.32}$$

where ϵ^{IJ} is the alternating symbol for $I, J = 1, 2$ with $\epsilon^{12} = 1$. Expression (4.32) is already very complicated to analyse for the most general edge configuration and again we refer to [18] for a comprehensive discussion. However, for the case of the graphs constructed in section 3 the situation becomes simple enough. Namely in this case the eight edges $e_{I\sigma\sigma'}$ have the property that $e_{I,sigma,\sigma'}$ and $e_{I,-\sigma,-\sigma'}$ are analytic continuations of each other. This implies that $\dot{e}_{I,\sigma,\sigma'}(0) = \sigma' \dot{e}_{I,\sigma\sigma',+}(0)$ where $e_{I\sigma\sigma'}(0) = v$ is the common starting point of all edges. Since $\epsilon(e, e', e'') = \text{sgn}(\det(\dot{e}(0), \dot{e}'(0), \dot{e}''(0)))$ is completely skew in e, e', e'', in this case we can simplify (4.32) to

$$\text{Vol}_0(v) = \sqrt{\left| \frac{1}{48 \cdot 64} \sum_{\substack{I_1, I_2, I_3 = 1,2 \\ \sigma_1, \sigma_2, \sigma_3, \sigma'_1, \sigma'_2, \sigma'_3 = \pm}} \epsilon(e_{I_1, \sigma_1 \sigma'_1, +}, e_{I_2, \sigma_2 \sigma'_2, +}, e_{I_3, \sigma_3 \sigma'_3, +}) \right.}$$
$$\left. \times [\sigma_1 \sigma'_1 \sigma_2 \sigma'_2 \epsilon^{I_1 I_2} + \sigma_1 \sigma'_1 \sigma_3 \sigma'_3 \epsilon^{I_3 I_1} + \sigma_2 \sigma'_2 \sigma_3 \sigma'_3 \epsilon^{I_2 I_3}] \right|} \tag{4.33}$$

Since (4.33) only depends on $\tilde{\sigma}_I = \sigma_I \sigma'_I$, after proper change of summation variables, (4.33) turns into

$$\text{Vol}_0(v) = \sqrt{\left| \frac{1}{48 \cdot 8} \sum_{\substack{I_1, I_2, I_3 = 1,2 \\ \sigma_1, \sigma_2, \sigma_3 = \pm}} \epsilon(e_{I_1, \sigma_1, +}, e_{I_2, \sigma_2, +}, e_{I_3, \sigma_3, +}) [\sigma_1 \sigma_2 \epsilon^{I_1 I_2} + \sigma_1 \sigma_3 \epsilon^{I_3 I_1} + \sigma_2 \sigma_3 \epsilon^{I_2 I_3}] \right|}$$
$$\tag{4.34}$$

Using that $\epsilon(e_{I_1,\sigma_1,+}, e_{I_2,\sigma_2,+}, e_{I_3,\sigma_3,+})$ and $\sigma_1\sigma_2\epsilon^{I_1 I_2}$ are both antisymmetric under the simultaneous exchange $(\sigma_1 I_1) \leftrightarrow (\sigma_2 I_2)$ etc. we may further simplify (4.34) to

$$
\begin{aligned}
\mathrm{Vol}_0(v) \;=\; & \sqrt{\Big| \frac{1}{48\cdot 4} \sum_{\sigma_1,\sigma_2,\sigma_3=\pm} \Big[\sum_{I_3} \sigma_1\sigma_2\, \epsilon(e_{1,\sigma_1,+}, e_{2,\sigma_2,+}, e_{I_3,\sigma_3,+}) + \sum_{I_1} \sigma_2\sigma_3\, \epsilon(e_{I_1,\sigma_1,+}, e_{1,\sigma_2,+}, e_{2,\sigma_3,+}) } \\
& \overline{ + \sum_{I_2} \sigma_3\sigma_1\, \epsilon(e_{1,\sigma_1,+}, e_{I_2,\sigma_2,+}, e_{2,\sigma_3,+}) \Big] \Big| }
\end{aligned}
\tag{4.35}
$$

Carrying out the respective sums over I_1, I_2, I_3 and using that $\epsilon(e, e', e'')$ is completely skew we can bring all orientation factors into one of the two standard forms $\epsilon(e_{1,\sigma_1,+}, e_{1,\sigma_2,+}, e_{2,\sigma_3,+})$ and $\epsilon(e_{2,\sigma_1,+}, e_{2,\sigma_2,+}, e_{1,\sigma_3,+})$ respectively. After proper relabelling of the σ_I we find that

$$
\mathrm{Vol}_0(v) = \sqrt{\Big| \frac{1}{16\cdot 4} \sum_{\sigma_1,\sigma_2,\sigma_3=\pm} \sigma_3 \left[\sigma_2\, \epsilon(e_{1,\sigma_1,+}, e_{1,\sigma_2,+}, e_{2,\sigma_3,+}) + \sigma_1\, \epsilon(e_{2,\sigma_1,+}, e_{2,\sigma_2,+}, e_{1,\sigma_3,+}) \right] \Big| }
\tag{4.36}
$$

Since $\epsilon(e_{I,\sigma_1,+}, e_{I,\sigma_2,+}, e_{J,\sigma_3,+})$ is skew in σ_1, σ_2 the sum over σ_2 collapses to the term $\sigma_2 = -\sigma_1$ and (4.36) becomes

$$
\begin{aligned}
\mathrm{Vol}_0(v) \;=\; & \sqrt{\Big| \frac{1}{16\cdot 4} \sum_{\sigma_1,\sigma_3=\pm} \sigma_3\,\sigma_1 \left[-\epsilon(e_{1,\sigma_1,+}, e_{1,-\sigma_1,+}, e_{2,\sigma_3,+}) + \epsilon(e_{2,\sigma_1,+}, e_{2,-\sigma_1,+}, e_{1,\sigma_3,+}) \right] \Big| } \\
\;=\; & \sqrt{\Big| \frac{1}{16\cdot 2} \sum_{\sigma_3=\pm} \sigma_3 \left[-\epsilon(e_{1,+,+}, e_{1,-,+}, e_{2,\sigma_3,+}) + \epsilon(e_{2,+,+}, e_{2,+,+}, e_{1,\sigma_3,+}) \right] \Big| }
\end{aligned}
\tag{4.37}
$$

Finally, using $\epsilon(e_{I,+,+}, e_{I,-,+}, e_{J,\sigma_3,+}) = \sigma_3\, \epsilon(e_{I,+,+}, e_{I,-,+}, e_{J,+,+})$ and $\epsilon(e_{1,+,+}, e_{1,-,+}, e_{2,-,+}) = \epsilon(e_{2,+,+}, e_{2,-,+}, e_{2,+,+}) = 1$ we find

$$
\mathrm{Vol}_0(v) = \frac{1}{2\sqrt{2}}
\tag{4.38}
$$

which does not agree with (4.30).

4.3 Discussion

Interestingly, for both valence $n = 4$ or $n = 8$ the expectation value is larger than the expected value with the same ratio $3/(2\sqrt{2})$. In general, for generic edge configurations and for higher and higher valence the expectation value will probably also be larger in ratio than the expected volume. This is because for a vertex of valence n the number of ordered triples of edges contributing to the expectation value is given by $\binom{n}{3}$ and for appropriate choice of the orientation factors, these terms all contribute with the same sign. Such a choice is always possible up to topological obstructions discussed to some extent in [18]. For large n the polyhedron dual to the vertex will approach more and more a sphere triangulated into n polygonal faces of typical unit area $4\pi/n$. Hence we expect the leading n behavior of the expectation value to be given by $\sqrt{\frac{1}{8}\, n^3/6\, (4\pi/n)^3} = \sqrt{8\pi^3/6} = 4\pi/3\sqrt{3\pi/4}$ while the expected volume should approach $4\pi/3$.

Surely, we have not shown that for graph topologies different from a cubical one the expectation value of the volume operator with respect to the dual cell complex coherent states cannot be matched with the classical volume value. This is because one can allow degenerate triples which decrease the volume expectation value. However, the discussion reveals that the question for which graphs the expectation value comes out correctly is far from trivial and even for natural choices the only admissible graph topology is the cubical one.

Notice that the expectation value is insensitive to the embedding of the graph relative to the dual cell complex as long as the graph is dual to it. For non dual embeddings or graph topologies which do not match the cell complex topology at all, the expectation value will be completely off the correct value. This demonstrates that the cut – off graph must lie within a certain class which is adapted to the cell complex.

5 Summary and Conclusions

Together with the analysis in [34] we have shown that the only known states of LQG which are semiclassical for the volume operator must be based on cubic cut – off graphs. This looks surprising at first but can maybe be understood intuitively as follows:

The volume operator is a derived operator and arises from the known representation of the flux operator on the Hilbert space. The derivation involves a regularization step which involves cubes surrounding the verticies of the graph in question on whose faces the fluxes are located. In order to take the limit in which the cubes shrink to the verticies and in order to make the result independent of the relative orientation between cubes and graphs, an averaging procedure must be applied. Hence one might be tempted to say that the fact that cubical topology is singled out rests on the cubical regularization.

However, this is not the case. Namely, cylindrical consistency and background independence alone already fix the cylindrical projections of the volume operator up to a global constant as proved explicitly in [8, 9]. The constant depends on the averaging procedure chosen and on whether one uses tetrahedra rather than cubes in the regularization. However, consistency between volume and flux quantization fixes that factor [10] and rules out the operator [8]. That is to say, there is no freedom left in defining the volume operator and therefore the details of the regularization do not matter, it is a regularization independent result. Hence, the preference for cubic graphs in the semiclassical analysis must have a different origin.

To see what it is, notice that the volume operator at a vertex involves a sum over ordered triples of edges adjacent to the vertex of which only the those with linearly independent tangents contribute. If the vertex has valence n then typically there are $\binom{n}{3}$ contributions [18]. They all contribute with equal weight (up to sign) which is the unique factor determined in [10]. That constant is such that each triple contributes as if (the tangents of) a triple of edges spans a corresponding parallelepiped. However, it is clear that generally far less than $\binom{n}{3}$ parallelepiped are sufficient to triangulate a (dual) neighborhood of the vertex and thus it is not surprising that large valence cut – off graphs will not give rise to good semiclassical states. On the other hand, unless the graph is cubic, even at low $n = 4$ the parallelepiped volume contribution per triple is too high for the triangulation of a tetrahedron. We have seen both effects at work in the previous section.

This result has two implications: Either one is able to find new types of states which are not constructed by the complexifier method or by different complexifiers than the ones employed so far such that the correct semiclassical behavior is recovered also for graphs of different than cubic topology. Or, if that turns out to be impossible, one should accept this result and conclude that, in order that the boundary Hilbert space of spin foam models has a semiclassical sector, one should generalize them to more general than simplicial triangulations of the four manifold as advocated in [32, 33].

References

[1] C. Rovelli. *Quantum Gravity.* (Cambridge University Press, Cambridge, 2004).

[2] T. Thiemann. *Modern Canonical Quantum General Relativity.* (Cambridge University Press, Cambridge, 2007).

[3] C. Rovelli. Loop quantum gravity, *Living Rev. Rel.* **1** (1998), 1. [gr-qc/9710008]
    A. Ashtekar and J. Lewandowski. Background independent quantum gravity: a status report. *Class.*

Quant. Grav. **21** (2004), R53. [gr-qc/0404018]

T. Thiemann. Lectures on loop quantum gravity. *Lect. Notes Phys.* **631** (2003), 41-135. [gr-qc/0210094]

[4] T. Thiemann. Anomaly-free formulation of non-perturbative, four-dimensional Lorentzian quantum gravity. *Physics Letters* **B380** (1996), 257-264. [gr-qc/9606088]

T. Thiemann. Quantum Spin Dynamics (QSD). *Class. Quantum Grav.* **15** (1998), 839-73. [gr-qc/9606089]

T. Thiemann. Quantum Spin Dynamics (QSD): II. The kernel of the Wheeler-DeWitt constraint operator. *Class. Quantum Grav.* **15** (1998), 875-905. [gr-qc/9606090]

T. Thiemann. Quantum Spin Dynamics (QSD): III. Quantum constraint algebra and physical scalar product in quantum general relativity. *Class. Quantum Grav.* **15** (1998), 1207-1247. [gr-qc/9705017]

T. Thiemann. Quantum Spin Dynamics (QSD): IV. 2+1 Euclidean quantum gravity as a model to test 3+1 Lorentzian quantum gravity. *Class. Quantum Grav.* **15** (1998), 1249-1280. [gr-qc/9705018]

T. Thiemann. Quantum Spin Dynamics (QSD): V. Quantum gravity as the natural regulator of the Hamiltonian constraint of matter quantum field theories. *Class. Quantum Grav.* **15** (1998), 1281-1314. [gr-qc/9705019]

T. Thiemann. Quantum Spin Dynamics (QSD): VI. Quantum Poincaré algebra and a quantum positivity of energy theorem for canonical quantum gravity. *Class. Quantum Grav.* **15** (1998), 1463-1485. [gr-qc/9705020]

T. Thiemann. Kinematical Hilbert spaces for fermionic and Higgs quantum field theories. *Class. Quantum Grav.* **15** (1998), 1487-1512. [gr-qc/9705021]

[5] T. Thiemann. The phoenix project: master constraint programme for loop quantum gravity. *Class. Quant. Grav.* **23** (2006), 2211-2248. [gr-qc/0305080]

T. Thiemann. Quantum spin dynamics (QSD): VIII. The master constraint. *Class. Quant. Grav.* **23** (2006), 2249-2266. [gr-qc/0510011]

[6] K. Giesel and T. Thiemann. Algebraic quantum gravity (AQG). IV. Reduced phase space quantisation of loop quantum gravity. [arXiv:0711.0119 [gr-qc]]

[7] M. Bojowald. Loop quantum cosmology. *Living Rev.Rel.* **8** (2005), 11. [gr-qc/0601085]

[8] C. Rovelli and L. Smolin. Discreteness of volume and area in quantum gravity. *Nucl. Phys.* **B442** (1995), 593-622. Erratum: *Nucl. Phys.* **B456** (1995), 753. [gr-qc/9411005]

[9] A. Ashtekar and J. Lewandowski. Quantum theory of geometry II: Volume operators. *Adv. Theo. Math. Phys.* **1** (1997), 388-429. [gr-qc/9711031]

[10] K. Giesel and T. Thiemann. Consistency check on volume and triad operator quantisation in loop quantum gravity. I. *Class. Quant. Grav.* **23** (2006), 5667-5691. [gr-qc/0507036]

K. Giesel and T. Thiemann. Consistency check on volume and triad operator quantisation in loop quantum gravity. II. *Class. Quant. Grav.* **23** (2006), 5693-5771. [gr-qc/0507037]

[11] T. Thiemann and O. Winkler. Gauge field theory coherent states (GCS): II. Peakedness properties. *Class. Quant. Grav.* **18** (2001), 2561-2636. [hep-th/0005237]

T. Thiemann and O. Winkler. Gauge field theory coherent states (GCS): III. Ehrenfest theorems. *Class. Quant. Grav.* **18** (2001), 4629-4681. [hep-th/0005234]

T. Thiemann and O. Winkler. Gauge field theory coherent states (GCS): IV. Infinite tensor product and thermodynamic limit. *Class. Quant. Grav.* **18** (2001), 4997-5033. [hep-th/0005235]

H. Sahlmann, T. Thiemann and O. Winkler. Coherent states for canonical quantum general relativity and the infinite tensor product extension. *Nucl. Phys.* **B606** (2001), 401-440. [gr-qc/0102038]

[12] T. Thiemann. Closed formula for the matrix elements of the volume operator in canonical quantum gravity. *Journ. Math. Phys.* **39** (1998), 3347-3371. [gr-qc/9606091]

[13] C. Rovelli and L. Smolin. Spin networks and quantum gravity. *Phys. Rev.* **D53** (1995), 5743-5759. [gr-qc/9505006]

[14] A. Ashtekar and C.J. Isham. Representations of the holonomy algebras of gravity and non-Abelian gauge theories. *Class. Quant. Grav.* **9** (1992), 1433. [hep-th/9202053]

A. Ashtekar and J. Lewandowski. Representation theory of analytic holonomy $C^\star$ algebras. In *Knots and Quantum Gravity*, J. Baez (ed.), (Oxford University Press, Oxford 1994). [gr-qc/9311010]

[15] J. Lewandowski, A. Okolow, H. Sahlmann and T. Thiemann. Uniqueness of diffeomorphism invariant states on holonomy – flux algebras. *Commun. Math. Phys.* **267** (2006), 703-733. [gr-qc/0504147]
C. Fleischhack. Representations of the Weyl algebra in quantum geometry. [math-ph/0407006]

[16] J. Brunnemann and T. Thiemann. Simplification of the spectral analysis of the volume operator in loop quantum gravity. *Class. Quant. Grav.* **23** (2006), 1289-1346. [gr-qc/0405060]

[17] A. R. Edmonds. *Angular Momentum in Quantum Mechanics*, (Princeton University Press, Princeton, 1974).

[18] J. Brunnemann and D. Rideout. Spectral Analysis of the Volume Operator in Loop Quantum Gravity. [gr-qc/0612147]
J. Brunnemann and D. Rideout. Properties of the volume operator in loop quantum gravity. I. Results. *Class. Quant. Grav.* **25** (2008), 065001. [arXiv:0706.0469 [gr-qc]]
J. Brunnemann and D. Rideout. Properties of the Volume Operator in Loop Quantum Gravity II: Detailed Presentation. [arXiv:0706.0382]

[19] K. Giesel and T. Thiemann. Algebraic quantum gravity (AQG) III. Semiclassical perturbation theory. *Class. Quant. Grav.* **24** (2007), 2499-2564. [gr-qc/0607101]

[20] H. Sahlmann and T. Thiemann. Towards the QFT on curved spacetime limit of QGR. 1. A general scheme. *Class. Quant. Grav.* **23** (2006), 867-908. [gr-qc/0207030]
H. Sahlmann and T. Thiemann. Towards the QFT on curved spacetime limit of QGR. 2. A concrete implementation. *Class. Quant. Grav.* **23** (2006), 909-954. [gr-qc/0207031]

[21] K. Giesel and T. Thiemann. Algebraic Quantum Gravity (AQG). I. Conceptual Setup. *Class. Quant. Grav.* **24** (2007), 2465-2498. [gr-qc/0607099]
K. Giesel and T. Thiemann. Algebraic Quantum Gravity (AQG). II. Semiclassical Analysis. *Class. Quant. Grav.* **24** (2007), 2499-2564. [gr-qc/0607100]

[22] T. Thiemann. Complexifier coherent states for canonical quantum general relativity. *Class. Quant. Grav.* **23** (2006), 2063-2118. [gr-qc/0206037]

[23] B. C. Hall. The Segal-Bargmann coherent state transform for compact Lie groups. *Journ. Funct. Analysis.* **122** (1994), 103-151.

[24] M. Varadarajan. Fock representations from U(1) holonomy algebras. *Phys. Rev.* **D61** (2000), 104001. [gr-qc/0001050]
M. Varadarajan. Photons from quantised electric flux representations. *Phys. Rev.* **D64** (2001), 104003. [gr-qc/0104051]
M. Varadarajan. Gravitons from a loop representation of linearised gravity. *Phys. Rev.* **D66** (2002), 024017. [gr-qc/0204067]
M. Varadarajan. The graviton vacuum as a distributional state in kinematic loop quantum gravity. *Class. Quant. Grav.* **22** (2005), 1207-1238. [gr-qc/0410120]

[25] A. Ashtekar and J. Lewandowski. Relation between polymer and Fock excitations. *Class. Quant. Grav.* **18** (2001), L117-L128. [gr-qc/0107043]

[26] A. Perez. Spin foam models for quantum gravity. *Class. Quant. Grav.* **20** (2003), R43. [gr-qc/0301113]

[27] E. Livine and S. Speziale. A New spinfoam vertex for quantum gravity. *Phys. Rev.* **D76** (2007), 084028. [arXiv:0705.0674 [gr-qc]]
J. Engle, R. Pereira and C. Rovelli. The Loop-quantum-gravity vertex-amplitude. *Phys. Rev. Lett.* **99** (2007), 161301. [arXiv:0705.2388 [gr-qc]]
E. Livine and S. Speziale. Consistently Solving the Simplicity Constraints for Spinfoam Quantum Gravity. [arXiv:0708.1915 [gr-qc]]
J. Engle, R. Pereira and C. Rovelli. Flipped spinfoam vertex and loop gravity. *Nucl. Phys.* **B798** (2008), 251-290. [arXiv:0708.1236 [gr-qc]]
L. Freidel and K. Krasnov. A New Spin Foam Model for 4d Gravity. [e-Print: arXiv:0708.1595 [gr-qc]]
J. Engle, E. Livine, R. Pereira and C. Rovelli. LQG vertex with finite Immirzi parameter. *Nucl. Phys.* **B799** (2008), 136-149. [arXiv:0711.0146 [gr-qc]]

[28] J. W. Barrett and L. Crane. Relativistic spin networks and quantum gravity. *J. Math. Phys.* **39** (1998), 3296-3302. [gr-qc/9709028]

J. W. Barrett and L. Crane. A Lorentzian signature model for quantum general relativity. *Class. Quant. Grav.* **17** (2000), 3101-3118. [gr-qc/9904025]

[29] S. Alexandrov. Simplicity and closure constraints in spin foam models of gravity. [arXiv:0802.3389 [gr-qc]]

[30] H. Sahlmann and T. Thiemann. Irreducibility of the Ashtekar – Isham – Lewandowski representation. *Class. Quant. Grav.* **23** (2006), 4453-4472. [gr-qc/0303074]
C. Fleischhack. Irreducibility of the Weyl algebra in loop quantum gravity. *Phys. Rev. Lett.* **97** (2006), 061302.

[31] E. Alesci and C. Rovelli. The Complete LQG propagator. I. Difficulties with the Barrett-Crane vertex. *Phys. Rev.* **D76** (2007), 104012. [arXiv:0708.0883 [gr-qc]]
E. Alesci and C. Rovelli. The Complete LQG propagator. II. Asymptotic behavior of the vertex. *Phys.Rev.* **D77** (2008), 044024. [arXiv:0711.1284 [gr-qc]]
V. Bonzom, E. Livine, M. Smerlak and S. Speziale
Towards the graviton from spinfoams: The Complete perturbative expansion of the 3d toy model. [arXiv:0802.3983 [gr-qc]]

[32] A. Mikovic. Spin Foam Perturbation Theory for Three-Dimensional Quantum Gravity. [arXiv:0804.2811 [gr-qc]]

[33] A. Baratin, S. Flori and T. Thiemann. The Holst Spin Foam Model on Cubulations. To appear.

[34] S. Flori and T. Thiemann. Semiclassical analysis of the Loop Quantum Gravity volume operator: Area Coherent States.

[35] J. Klauder and B.-S. Skagerstam. *Coherent States*, (World Scientific, Singapore, 1985).

[36] T. Thiemann. Reality conditions inducing transforms for quantum gauge field theories and quantum gravity. *Class. Quant. Grav.* **13** (1996), 1383-1403. [gr-qc/9511057]

[37] A. Ashtekar, J. Lewandowski, D. Marolf, J. Mourão and T. Thiemann. Quantisation of diffeomorphism invariant theories of connections with local degrees of freedom. *Journ. Math. Phys.* **36** (1995), 6456-6493. [gr-qc/9504018]

[38] A. Ashtekar, J. Lewandowski, D. Marolf, J. Mourão and T. Thiemann. Coherent state transforms for spaces of connections. *Journ. Funct. Analysis.* **135** (1996), 519-551. [gr-qc/9412014]

[39] O. Bratteli and D. W. Robinson. *Operator algebras and quantum statistical mechanics*, vol. 1,2, (Springer Verlag, Berlin, 1997).

[40] A. Ashtekar and J. Lewandowski. Projective techniques and functional integration for gauge theories. *J. Math. Phys.* **36** (1995), 2170-2191. [gr-qc/9411046]

[41] A. Ashtekar and J. Lewandowski. Quantum theory of geometry I: Area Operators. *Class. Quant. Grav.* **14** (1997), A55-A82. [gr-qc/9602046]

[42] B. Bahr and T. Thiemann. Gauge-invariant coherent states for Loop Quantum Gravity. I. Abelian gauge groups. [arXiv:0709.4619 [gr-qc]]
B. Bahr and T. Thiemann. Gauge-invariant coherent states for loop quantum gravity. II. Non-Abelian gauge groups. [arXiv:0709.4636 [gr-qc]]

[43] J. Velhinho. A groupoid approach to spaces of generalised connections. *J. Geom. Phys.* **41** (2002), 166-180. [hep-th/0011200]
J. Velhinho. On the structure of the space of generalised connections. *Int. J. Geom. Meth. Mod. Phys.* **1** (2004), 311-334. [math-ph/0402060]
B. Bahr and T. Thiemann, Automorphisms in loop quantum gravity. [arXiv:0711.0373 [gr-qc]]